Title
C. elegans glial HSF-1 protects from stress and aging via a novel neural mechanism

Author
Gildea, Holly Katherine

Publication Date
2022

Peer reviewed|Thesis/dissertation

C. elegans glial HSF-1 protects from stress and aging via a novel neural mechanism

By

Holly Katherine Gildea

A dissertation submitted in partial satisfaction of the

requirements for the degree of

Doctor of Philosophy

in

Neuroscience

in the

Graduate Division

of the

University of California, Berkeley

Committee in charge:

Professor Andrew Dillin, Chair
Professor Helen Bateup
Professor Kaoru Saijo
Professor Gloria Brar

Spring 2022

Abstract

C. elegans glial HSF-1 protects from stress and aging via a novel neural mechanism

by

Holly Katherine Gildea

Doctor of Philosophy in Neuroscience

University of California, Berkeley

Professor Andrew Dillin, Chair

This work addresses two major unsolved questions in the field of *C. elegans* neuroscience and stress biology. First, are glia of the worm able to regulate the heat shock response (HSR) in a non-cell autonomous manner? Second, are these glia also required for regulation of such a response?

In the first chapter, I introduce concepts relevant to the works herein presented. Aging induces cellular dysfunction partially by the decline of protein homeostasis stress responses. When this function is restored, animals live longer and healthier. Although stress responses are specialized to the functions of individual organelles, signaling can be transmitted from neural cells to peripheral tissues in a protective manner. The role for glia, the non-neuronal cells of the brain, in this process is not well described. Glia, including astrocytes, closely regulate homeostasis of brain tissues, including by immune and stress responses. As this homeostasis deteriorates with age, risk of neurodegenerative disease increases. Most neurodegenerative diseases are characterized by the accumulation of protein misfolding, including Alzheimer's Disease (AD). AD patients, among those with other so-called "tauopathies," exhibit misfolding of the microtubule-associated protein tau. Tau abnormalities are associated with neuronal dysfunction, but their role in organellar stress response induction has not been well characterized.

In the second chapter, I examine the mechanism by which the cephalic sheath (CEPsh) glia of the nematode *C. elegans* coordinate the HSR across tissues to increase stress resistance, lifespan, and immune tolerance. When the main regulator of the heat shock response, heat shock factor 1 (*hsf-1)*, is over-expressed in the four CEPsh cells, I identify an increase in lifespan alongside peripheral induction of heat shock chaperones and an increase in heat stress tolerance. The mechanism by which this non-cell autonomous communication occurs is independent of the neuronally-coordinated HSR system, operating without requirement for the AIY interneuron or serotonin synthesis. The response is also transmitted independent of previous glial-derived signals, which had originated from UNC-31-mediated dense core vesicles, and instead relies on transmission by UNC-13-mediated small clear vesicles. However, there is no clear requirement for a singular neurotransmitter that might be contained in such vesicles. In the periphery, *hsf-1* itself is required, as the insulin signaling factor *daf-16* in a partial manner. In addition, immune factors are highly upregulated in CEPsh glial *hsf-1* animals, which are resistant to pathogenic

bacteria. Taken together, I here identify a unique signaling mechanism by which CEPsh glia specifically modulate heat stress signaling.

In the third chapter, I investigate the endogenous role for CEPsh glia in regulation of the HSR. I first characterized by imaging several types of developmental mutants causing CEPsh glial ablation. I next tested these strains for heat stress tolerance and found that mutants for the development of all four CEPsh cells, but not ventral CEPsh glia alone, displayed increased thermotolerance relative to wild type animals. This did not occur concomitant with increased chaperone induction. Further, I identified a requirement for CEPsh glia in neuronal HSR signaling, for both lifespan extension and for thermotolerance induction. These data suggest that CEPsh glia are naturally strong regulators of the heat shock response, and that such regulation may occur in a positive and negative fashion, in close interaction with neurons. More work is necessary to understand the dynamic nature of this regulation, and through what mechanism it occurs in the glial and neuronal systems.

In sum, I here describe several unique roles and signaling mechanisms concerning the heat shock response for the CEPsh glia of *C. elegans*. These data, in combination with prior works, demonstrate that CEPsh glia flexibly and specifically respond to organelle-targeted stressors, coordinating an organismal response to that unique cue. In the case of heat stress, such cues may include heat or other protein misfolding insults, as previously shown, but also pathogen stress. Further, CEPsh cells serve a larger role supporting neuronal HSR signaling, which remains unprobed. Taken together, I show that CEPsh glia are both sufficient to regulate organismal heat stress and necessary to ensure endogenous HSR function range. These works will shed light on how neuronal and glial aging impact organismal health and longevity, particularly in the case of neurodegenerative diseases.

Table of Contents

Figures and Tables

Main Figures

Supplementary Figures

Tables

Acknowledgements

This work would not have been possible without the support and efforts of many incredible people. Though it would be impossible to name them all, here are just a few.

Thank you first to the whole Dillin Lab, and to Andy specifically, for allowing me to forge my own path in my work and teaching me so much about how to advocate for myself alongside my science. I am incredibly grateful for the innumerable collaborations and constructive conversations I have had in the lab over the years. Thank you particularly to the Dillin lab-derived friends who have become a much larger part of my life- we truly are a funky bunch! I owe many thanks particularly to my mentors in the lab. To Ashley, whose mentorship and guidance made me into the scientist I am today, thank you for always going above and beyond. Thanks also to Koning and Cory whose scientific mentorship kept me sane, realistic, and evaluative, and whose friendship has given me the joy and sense of belonging to show up to lab even when it felt impossible. It is an incredible blessing to have you both in my life. Thank you to Camila and Samira for helping me feel understood, for the perspective that the future is worth fighting for, and for a refusal to live in "moderation." Thank you to Melissa for gelato escapes, elite Illustrator skills, and the "S" energy my "N" vibes need. Thank you to Phil for being my partner in crime in the Dillin Lab since day one; I'm incredibly grateful of course for your scientific investment in my work, but mostly for your care in me as a person and encouragement through the bad times in grad school alongside the good times. I am blessed to have you all as friends.

Thank you to my committee for help and insightful comments throughout this process.

Thank you to my mentees, Helen, Tayla, Shannon, the students I taught in class, and the younger graduate students who looked to older graduate students for support. Your scientific contributions are clear, but beyond that your personal impacts make science better. I deeply appreciate all you taught me. I hope that academia continues to improve in your time.

Thank you to the "Basal Gang," Jacob, Zuzanna, Bill, Kevin, Christine, Vael Gates, Tobias, and Carson, my neuroscience cohort, and all HWNI and MCB friends (Rebecca, Celia, and everyone) for support and fun throughout grad school. Thanks to the Helen Wills community as a whole, especially the staff who make the neuroscience program possible. Thank you to the many professors who invested energy in my scientific development and encouraged my ideas.

Thank you to Alex Jaworski and the whole Jaworski lab for giving me my first chance to become a scientist. I would not be here today without that chance, in addition to all the feedback, patient conversations, and excitement about data that followed. To paraphrase a tweet, academics either have a family history of getting PhDs or one professor who believed in them when they didn't deserve it and helped them pursue their dreams. I am very lucky to fall into the latter category.

Thank you to all members of the glia research community, who welcomed me without hesitation and allowed me to be my full self. I am grateful to be part of one of the most inclusive fields in neuroscience and hope to learn alongside you all for many years to come.

Thank you to non-Berkeley friends- to Haley, Marcy, Mariana, Bella, Naina, Katie, Vivian, and Nicole for being your own incredible selves, encouraging me to do the same, and always being ready to spring into action when I needed you. Thanks to the “Husbands” to our Abe’s Babes for loving and supporting us all.

Thank you to the Evans family, who have loved me as your own and stood up for me since the very beginning. I am so lucky to be a part of your family.

Thank you to my family for being my first spark to pursue science and for cultivating a spirit of resilience without which this degree would not have been possible.

Finally, to my fiancé Abe, who has been my staunchest supporter in this journey from the beginning: this would truly be impossible without you, and I count myself among the luckiest people alive to have you by my side. From delivering cookies to my first diaphragm dissections when we were 19, through late nights in lab falling asleep at my desk, I have never felt more encouraged, defended, and inspired in life than by you. This degree also belongs in part to you, as you have felt its struggles and joys in full. Thank you for loving the joy I take in my work.

Chapter 1: Introduction

Protein Quality Control

As organisms age, damage accumulates that can cause cellular dysfunction. However, in addition to the experience of cell stress over a lifetime, the cellular ability to mount a response to stress also declines over time(*1*, *2*). In the case of protein toxicity this example is particularly poignant. Cells have developed compartment-specific responses to detect protein folding mishaps, temporarily limit production, and upregulate protective chaperones that rescue the cell from potential toxic aggregates (*3*). Although early philosophies of aging identified aggregate-related damage accumulation as the central problem, recent work suggests that protein misfolding naturally occurs across an organism's lifetime and is rescued by cellular stress responses (*4*). Stress responses, however, become less effective with age, leading to a failure to resolve damage (*1*, *2*). In fact, rescue of function for these responses by overexpression of their effectors has been shown to increase healthspan and lifespan, indicating that unfolded protein responses themselves are a potential therapeutic target for aging (*1*, *5*, *6*).

Cellular quality control of protein folding is essential, and the process by which cells maintain protein homeostasis is known as "proteostasis" (*7*). Protein conformations are required for their functions. When incorrectly folded, proteins can also aggregate forming toxic oligomers and larger inclusions and plaques, which can cause cellular damage and dysfunction. Misfolded proteins are common features of aging, particularly in the brain, where their presence is associated with many aging-related neurological diseases(*7*). Alzheimer's Disease presents with aggregates of the microtubule-associated protein tau intracellularly and amyloid beta aggregates extracellularly; Parkinson's Disease is associated with the accumulation of misfolded alpha-synuclein, and Huntington's Disease with misfolded poly-glutamine repeat expansions (*8*, *9*). Such neurodegenerative diseases share several common features, among which one is the highlighted protein misfolding characteristics, and another that age is the biggest risk factor for their development (*9*). Our study of aging-related dysfunction of protein misfolding is therefore paramount in the mechanistic understanding and future treatment of these diseases.

To prevent misfolding, cells employ proteins called "chaperones," which guide nascent peptides through the folding process (*10*). If protein production works as an assembly line, as each peptide goes through translation, folding, modification, and export to its destination, then chaperones serve as the line's quality control staff, binding and releasing peptides as they assume the proper conformation. However, when the assembly line and quality control chaperones are overwhelmed, in some instances by a large increase in translation or by external stimuli such as heat that can induce misfolding, the cell must induce an alarm system to slow or stop the assembly line and increase available numbers of chaperone staff. These alarm systems are known as unfolded protein responses (UPRs) (*11*, *12*). Cellular compartments initiate unique UPR signaling cascades upon stress. Such alarm and response systems are available in all compartments in which protein folding occurs- in the endoplasmic reticulum (ER), the mitochondria, and the cytosol.

Unfolded Protein Responses

Overall, UPRs take similar forms across organelles, despite initiating distinct signaling pathways. Usually, a sensor responds to the presence of a misfolded protein or similar insult,

subsequently leading to the activation of a UPR-specific transcription factor. That transcription factor then translocates into the nucleus to upregulate sets of genes that work to resolve stress of the specific organelle. Chaperone upregulation and reductions of load on the system, either by decreasing translation or by increasing organellar function through other means, are common response components.

In the ER, the UPR (UPR^{ER}) is activated in response to sensing of misfolded proteins or lipid stress by three transmembrane factors: inositol-requiring enzyme 1 (IRE-1), activating transcription factor 6 (ATF6), and protein kinase RNA-like ER kinase (PERK) (*11*). IRE-1 when activated causes the non-canonical cleavage of an unconventional intron in the *xbp-1* mRNA sequence, leading to a spliced version called *xbp-1s*, which is then translated and translocates into the nucleus to enact its transcription factor functions (*11*). XBP-1 then upregulates ER chaperones and other protective genes to increase ER function and resolve stress (*11*). ATF-6 when activated is shuttled to the Golgi apparatus, cleaved, and can then translocate into the nucleus to upregulate similarly protective genes, including those involved in ER-associated degradation (ERAD) to aid in misfolded protein clearance (*11*). PERK activation, in contrast, initiates downstream signaling by phosphorylating the translation initiation factor eIF2α, causing a decrease in overall translation initiation (*11*). Under these conditions, some transcripts, including activating transcription factor 4 (ATF-4), are preferentially translated, the downstream signaling of which can lead to induction of apoptosis if the UPR^{ER} fails to resolve stress (*11*). Overall, XBP-1 and ATF-6-mediated pathways are shorter acting than PERK signaling; thus, the cell can either rapidly resolve a stress, or if chronic, instead induce apoptosis (*13*, *14*). Of all three branches, the IRE-1 mediated branch is the best conserved, present from yeast (via the IRE-1 homolog HAC1) through to humans, although PERK and ATF-6 exist in invertebrates as well as vertebrates (*3*).

In the mitochondria, the UPR (UPR^{mt}) relies primarily on the transcription factor ATFS-1 (*12*, *15*). Under basal conditions, ATFS-1 is imported into the mitochondria and is subsequently degraded (*15*). However, when mitochondrial stress occurs, which perturbs import, ATFS-1 gets rerouted to the nucleus, where it functions as a transcription factor to upregulate chaperones, import machinery, and other factors to rescue mitochondrial stress (*15*). Prolonged unresolved mitochondrial stress, however, can lead to mitochondrial degradation via mitophagy (*15*). Though initially discovered in mammals, the UPR^{mt} serves important roles in invertebrates such as *C. elegans* (*15*).

In the cytosol, the UPR is known as the heat shock response (HSR) and is primarily mediated by the transcription factor heat shock factor 1 (HSF-1) (*16*). Although several other HSFs exist in mammals, while invertebrates express just HSF-1, in all cases HSF-1 remains the primary HSR regulator (*12*). HSF1 and HSF2 have the ability to activate the HSR in mice, and HSF4 is involved in some development of some neurons (*12*). Under basal conditions, HSF-1 exists in its monomeric form in the cytosol, bound by chaperones HSP-70 and HSP-90 in an inhibitory manner. When improperly folded proteins are detected in the cytosol, they titrate HSP-70 and HSP-90 away from binding HSF-1, which frees the transcription factor to trimerize , become phosphorylated, and translocate into the nucleus (*16*). HSF-1 then targets loci for transcription at least in part by using the heat shock element (HSE) sequence. HSF-1 activity upregulates heat shock chaperones, including HSP-70, to aid protein folding and resolve the

stress (*5*, *16–18*). Heat has been used in the literature as a stressor to induce cytosolic protein misfolding, and thus the HSR. For this reason, many major chaperones used in this and other UPR pathways are designated with the prefix "HSP," meaning "heat shock protein," as they are upregulated under heat stress conditions.

UPRs in the *C. elegans* Model System

The small transparent nematode *C. elegans* is a compelling system for the study of neural functions and of stress responses. In the worm, adult cells are all post-mitotic, excepting the germline, and have a pre-specified orientation relative to all other cells, allowing for a whole-animal cell by cell map. This is particularly useful in the case of neurons and other neural cells, as the entire connectome of the animal has been mapped (*19*). Further, the animals have a relatively short average lifespan, allowing for study of aging. They are also genetically tractable, with mutable genomes and easy treatment by RNA interference (RNAi) (*20*). Worms can exist as self-crossing hermaphrodites or males, making genetic crosses feasible. The adult hermaphrodite has 959 somatic cells, 302 neurons, and 56 glia (*21*). Worms are particularly useful for the study of the stress responses introduced above (*22*).

Interestingly, UPR functions decline as animals age, on the level of gene expression of UPR components, post-translational modifications/ localization of the same, and in ease of activation and signaling (*1*, *2*, *23*, *24*). In the *C. elegans* model system, this decline has been shown for the UPR^{ER} and the HSR specifically (*1*)(*2*). HSR down-regulation occurs as a programmed event as worms reach maximum reproductive capacity, suggesting that parent animals prioritize progeny proteostasis pathways over their own UPR functions (*2*). The aging-related decline in proteostasis functions is associated with worsening protein aggregation (*25*). Further, rescue of UPR function is sufficient to decrease protein aggregation (*1*, *18*, *26*). These data suggest UPRs as a potential druggable target for aging-related diseases of protein aggregation.

Neuronal Aging and Susceptibility

As noted above, neurological diseases of aging are often characterized by neuronal protein misfolding. Why might neurons, in particular, be sensitive to this type of dysfunction? Cellular age may be one factor, as neurons exist in a post-mitotic state after their initial specification, some for an entire human lifetime (*27*). Although adult neurogenesis is possible, its products are rare relative to total neuronal number, and thus overall, the neurons of an older person are older themselves (*27*, *28*). Post-mitotic cells additionally lose the opportunity to jettison protein aggregates when dividing, instead relying on effective proteostasis maintenance throughout the cellular lifetime (*27*, *29*).

Neurons also face a distinct diffusion problem. Neuronal somata are often located considerable distances from their most distal processes. In the case of the longest spinal cord-derived axons in humans, this distance can be up to a meter – far too long a distance for organisms to manage protein stress with slow-moving axonal transport. Similarly, even when diffusion is not limited by distance it is often limited by space, in the case of dendritic spines and

other sub-process compartments. It is infeasible for neurons to independently enact transcription-dependent responses in the case of synaptic proteins or local translation functions.

This problem led to a central UPR function question: Do neurons induce UPRs purely cell autonomously, or are they able to recruit responses from other cells and tissues? Research concerning the UPR^{mt}, UPR^{ER}, and the HSR all demonstrate that neurons can induce UPRs non-cell autonomously, in peripheral tissues such as the intestine (*1*, *5*, *6*, *30*). Indeed, this UPR induction rescues protein misfolding and improves the lifespan of neuronal UPR-increased animals (*1*, *5*, *6*, *30*).

The Neuronal Heat Shock Response

Particularly in the case of the HSR, such findings established a neuronal signaling mechanism and downstream metabolic changes necessary both for the peripheral communication of the response and its stress tolerance and lifespan benefits (*5*). *C. elegans* require thermosensory neurons to induce peripheral heat shock response phenotypes in response to heat sensing, implying that non-autonomous communication regulates HSR levels across the organism (*17*). This sensing and signaling is dependent at least on two cells in the thermosensory circuit: the directly heat-sensing neuron AFD and its downstream interneuron AIY (See Figure 2A) (*17*). Defects in *gcy-8*, necessary for heat transduction by AFD, or in *ttx-3*, necessary for signaling by AIY, both abrogate the peripheral chaperone increase upon heat stress and decrease survival under heat stress conditions (*17*). Notably, however, my work since suggests that this strict regulation of chaperone induction depends on timing and severity of heat insult (See Figure 2). The authors also point out that dauer hormone, secreted from starved developmentally arrested *C. elegans* animals, highly potentiates the HSR in *gcy-8* mutant animals (*17*). These data suggest that the HSR is not just activated by neurons, but rather is dynamically sensed and controlled by the nervous system in a context dependent manner.

The AFD neuron can activate or inhibit HSR function through activity of a downstream circuit, which prior work has found to converge on serotonin (*18*). Through stimulation of the AFD neuron using optogenetics, Tatum et al. demonstrated that electrical activity of this neuron is correlated to intestinal activation of HSF-1, measured by visualization of HSF-1 protein in the nucleus (*18*). This work also found AFD activation led to downstream release of the monoamine neurotransmitter serotonin, and that mutation of serotonin synthesis, via mutation of the tryptophan hydroxylase enzyme gene *tph-1*, led to a partial knockdown of heat-dependent chaperone induction (*18*). Optogenetic activation of serotonergic neurons also seems to induce a peripheral HSR (*18*). Thus emerged the model in which the thermosensory circuit works via heat transduction into electrical signal by AFD, followed by activation of its synaptic partner AIY, which in turn activates serotonergic signaling. The ability of neurons to non-autonomously communicate the HSR was thus established.

These initial works demonstrated that neuronal electrical activity could be coupled to downstream cellular responses, a new conception of what sensory input may mean for organisms. Typically, sensory systems convert relevant inputs into electrical stimulation in neurons, those neurons communicate with other cells to generate sensation, additional cells are recruited to plan an appropriate motor action, and then downstream cells are activated to produce

a behavioral response. In this case, though the response remains cue-appropriate, sensation leads not to a motor behavior but instead to a cellular behavior, the induction of the HSR. As we appreciate the connection between UPRs, cellular heath, and organismal longevity, these concepts pose interesting avenues to expand our conception of the role of the nervous system.

When *hsf-1* is over-expressed in all 302 neurons of the worm, about one third of its total cells, animals are both long-lived and more heat tolerant than wild type animals (*5*). This leads to peripheral induction of metabolic changes, for example, in the insulin signaling pathway, which has been highly correlated with lifespan (*5*). Moreover, *hsf-1* expression in neurons seems to be uniquely protective, as expression in other tissues, such as the intestine and muscle, does not robustly increase lifespan (*31*, *32*). The neuronal *hsf-1* overexpression model relies on *daf-16*, an insulin signaling transcription factor, in the intestine to enact its lifespan extension, suggesting that metabolic coupling between neurons and intestine leads to healthier phenotypes (*5*). Interestingly, however, though the lifespan phenotypes are mediated by *daf-16*, they are independent of the thermosensory circuit neuron AIY, via *ttx-3* mutation (*5*). In contrast, the heat stress tolerance phenotypes conveyed by neuronal *hsf-1* do depend on AIY, but not on *daf-16* (*5*). The two phenotypes of lifespan and stress tolerance thus seem to originate from distinct neuronal mechanisms, likely the first through the AFD-AIY-serotonin pathway, and the second through an unknown mechanism.

Interestingly, serotonin seems to serve as a stress-sensing node in *C. elegans*. Non-cell autonomous communication of the HSR from neurons at least in part, relies on its use (*5*, *18*, *33*). Serotonin also serves a role in UPR^{mt} signaling by neurons and in UPR^{ER} signaling by neurons, though in both cases other factors can contribute to downstream peripheral changes (*34*, *35*). Despite diverging downstream consequences and distinct transcription factors over-expressed for their induction, each neuronal UPR somehow alerts the serotonergic system in order to signal to other tissues.

Having established that neurons certainly have the ability to signal non-cell autonomously concerning heat stress, several questions remain concerning their endogenous responsiveness and HSR function. HSF1 function is organismally required for neuronal survival, as null mutant animals experience severe neurodegeneration (*36*). However, when neurons are under misfolded protein stress during aging-related degenerative disease, in the cases of Alzheimer's Disease and Huntington's Disease, HSF1 protein is degraded for reasons that are not fully understood (*24*, *25*). Further, neurons themselves do not seem to be the most efficient HSR-inducing cells of the brain (*24*, *25*, *37*, *38*). Therefore, despite the critical nature of the HSR in neuronal health and survival, these problems and the unique neuronal proteostasis problems mentioned above require that they recruit assistance in HSR function.

Glia

Luckily neurons are not unsupported inhabitants of the brain parenchyma. The non-neuronal cells of the brain, glia, serve to support and direct electrical, metabolic, and homeostatic functions of neurons across many modalities (*39*, *40*). Neurons use an incredible amount of energy to initiate action potentials, and must be supplied with ions, neurotransmitters, and metabolic support to function (*41–43*). Glia both serve these roles and additionally coordinate

neural activity, coordinate permeability of the blood brain barrier, provide survival/ trophic cues to neurons, handle inflammatory responses and synaptic wiring, and more (*40*, *44*, *45*).

In mammals, central nervous system glia fall into three main categories, though more cell types exist particularly at the blood brain barrier. Oligodendrocytes regulate survival of neurons via secretion of growth factors, throughout development and adulthood (*45*). They also ensheath neuronal processes in their many-layered myelin wraps, which serve to increase neuronal conduction velocity as does a wrap on a wire (*45*). Microglia are known best as the resident macrophages of the brain, which activate nearly all inflammatory processes and mediate most brain immune signaling (*40*). They also use their phagocytic functions to shape neuronal processes in an activity-dependent manner, known as synaptic pruning (*40*). Microglial pruning is best described during development but has also been demonstrated in the removal of dysfunctional synapses in neurodegeneration (*46*, *47*). Phagocytosis by microglia is also responsible for clearance of brain debris, including myelin, protein aggregates, or other damage products (*40*). Finally, astrocytes accomplish most metabolic signaling in the brain (*44*). These cells are intimately connected to the blood brain barrier, regulating what factors can enter or exit in a dynamic manner. Astrocytes are also highly metabolically coupled to neurons, providing lactate in particular to aid in ATP production for energy costly neurons (*42*). Recent work suggests that astrocytes are also efficient mediators of neuronal organelle health and proteostasis. Neurons may directly shuttle damaged organelles and misfolded proteins to astrocytes (*48*, *49*). They are also particularly responsive under HSR induction conditions, to a greater extent than neurons (*37*, *38*, *50*).

Glia in Proteostasis

Recent work in *C. elegans* suggests glia play a larger role in proteostasis maintenance for their fellow cells (*26*, *51*). Worms have 56 glial cells, four of which, known as the cephalic sheath, or CEPsh, cells, closely resemble mammalian astrocytes (*21*). These cells support neuronal development and form tripartite synapses to provide neurotransmitter and metabolic support to neurons (*21*). CEPsh glia are poised at a unique junction of the periphery and the nervous system. CEPsh glia ensheath processes of sensory neurons that project their endings into the environment (*52*). They also surround the nerve ring, forming a prototypical barrier between the central nervous system and the rest of the body (*52*).

Interestingly, recent work demonstrates that CEPsh glia over-expressing the UPR^{ER} transcription factor *xbp-1s* can induce lifespan extension, ER stress tolerance, and non-cell autonomously induce the UPR^{ER} (*26*). Surprisingly, the mechanism by which this occurs is completely independent from the neuronal non-autonomous signaling pathway, which uses small clear vesicles, likely transporters of neurotransmitters (*1*, *26*). Instead, CEPsh glial UPR^{ER} relies on dense core vesicles, which carry larger cargos, and neuropeptide synthesis, likely from CEPsh glia themselves (*26*). Similarly, a non-cell autonomous signaling mechanism for a pan-glial-derived UPR^{mt} was found to rely on neuropeptides (*51*). Thus, *C. elegans* glia both can induce protective non-cell autonomous UPR responses and converge on a different signaling mechanism than that of neurons, instead using neuropeptides via dense core vesicles.

In the UPR^{ER} and UPR^{mt}, neuronal signaling mechanisms are well established, however, *C. elegans* glia contribute a new angle of proteostasis management for the organism (*1*, *5*, *6*, *26*, *30*, *34*, *35*, *51*, *53*, *54*). In the HSR, where there are certainly at least two pathways at play, neither of which are fully defined, no one has yet examined the role of CEPsh glia. This work attempts to answer two major questions derived from this concept. One, can CEPsh glia accomplish non-cell autonomous signaling of the HSR, and with what effect on organismal health? Two, what is the endogenous role of CEPsh glia in heat sensing and signaling, and could this function be required for neuronal HSR signaling or health?

Taken together, glial proteostasis is an important avenue of study to understand how aging impacts the brain, and neurons in particular. Astrocytes, and in the case of *C. elegans*, CEPsh glia, maintain not only homeostasis of neuronal energy states and signaling, but also maintain proteostasis in an integrated mechanism of cellular sensation. An increasing body of work in this field will open up new biological understandings of brain protein misfolding alongside an increase in relevant therapeutics for aging and neurodegeneration.

Chapter 2: Glia of C. elegans coordinate the heat shock response independent of the neuronal thermosensory circuit and serotonin

This chapter contains previously published material from the following work, and permissions have been obtained from all co-authors for inclusion in this document

Gildea HK, Frankino PA, Tronnes SU, Pender CL, Choi HO, Cheung S, Hunter T, Dillin A. Glia of *C. elegans* coordinate the heat shock response independent of the neuronal thermosensory circuit and serotonin. *Biorxiv* January 31, 2022.

Introduction:

Cellular insults occur as animals age that can cause dysfunction. Cells have compartment-specific signaling pathways that detect such insults, temporarily limit protein production, and upregulate protective genes, such as the protein folding assistant chaperones, to rescue cells from potentially toxic protein misfolding. As organisms experience damage over a lifetime, the cellular ability to mount responses to stress also declines (*1*, *2*). The process of aging perturbs cellular homeostasis by reducing organelle-specific unfolded protein response (UPR) induction and efficacy (*1*, *2*). Rescue of UPR functions by over-expression of activators in the nervous system increases healthspan and lifespan, indicating that UPRs are a potential therapeutic target for aging (*1*, *5*, *30*).

The compartment-specific UPR initiated by proteotoxic stress in the cytosol is known as the heat shock response (HSR) and is primarily mediated by the highly conserved transcription factor heat shock factor 1 (HSF-1) (*12*). Under non-stressed conditions, chaperones such as HSP-70 and HSP-90 bind HSF-1, suppressing its activation (*55*). Upon detection of misfolded proteins in the cytosol the chaperones are titrated away from HSF-1, freeing the transcription factor to trimerize and translocate into the nucleus (*55*). There, HSF-1 upregulates chaperones and other genes that help resolve stress. HSF-1 activity declines with age, and this dysfunction occurs concomitant with worsening of cytosolic protein aggregation (*2*, *24*, *25*).

Recent work has established a unique role for the nervous system in initiating UPRs, including the HSR, across the whole organism (*1*, *5*, *17*, *18*, *30*, *53*). When the 302 neurons of *C. elegans* over-express *hsf-1*, animals exhibit a non-cell autonomous activation of the HSR in peripheral tissues, which leads to an increase in thermotolerance and lifespan (*5*). In *C. elegans*, heat sensing occurs via the canonical thermosensory circuit including AFD, AIY, and serotonergic neurons, and is required for behaviors such as thermotaxis, although some other neurons can contribute to heat-related behaviors (*56*). Interestingly, electrical activation of AFD sensory neurons and downstream ADF serotonergic neurons has been shown to induce peripheral HSF-1 activation in addition to canonical heat sensing behaviors, and this circuit has a demonstrated role in non-cell autonomous HSR signaling (*5*, *18*, *57*). Thus, neural activity due to the sensory experience of heat, a potentially damaging insult, is coupled to the relevant organismal intracellular heat shock stress response.

Despite neuronal ability to induce the HSR non-cell autonomously when exogenously activated, neurons are likely not the most potent responders of the nervous system (*24*, *25*, *37*, *38*). Hyperthermia induces chaperone expression in neural cells; however, glia, particularly astrocytes, upregulate chaperones more robustly than neurons in these conditions (*37*, *38*). *In vitro* data suggest that glia may even provide chaperones to neurons directly (*50*). Neurons also aberrantly degrade HSF1 in several neurodegenerative disease conditions, including Alzheimer's and Huntington's Diseases, in model organisms, and in human tissue (*24*, *25*). These findings suggest that glia, not neurons, are likely the primary coordinators of cytosolic stress responses in the nervous system.

C. elegans glia play an important role in regulation of cellular stress and longevity (*26*, *51*). The 56 glia of *C. elegans* perform classic glial functions, supporting neuronal development,

participating in synapses, and providing neurotransmitter and metabolic support to neurons (*21*, *52*). Four of these cells, the cephalic sheath (CEPsh) glia, most closely resemble mammalian astrocytes (*21*). CEPsh glia are poised at a unique junction of the environment, peripheral tissues, and the nervous system. They ensheath processes of sensory neurons that project their endings into the environment. These glia also surround the nerve ring, forming a barrier between the nerve ring and the rest of the body (*52*). Recent work has demonstrated that these cells are able to induce organelle-specific stress responses non-cell autonomously in the case of the endoplasmic reticulum (ER) and mitochondria, but their role in cytosolic protein stress sensing and signaling has not been explored (*26*, *51*).

Here, we find that over-expression of *hsf-1* in the four CEPsh glia of *C. elegans* is able to coordinate an organismal HSR, confer stress resistance, and extend lifespan. Signaling of the glial HSR relies on a mechanism distinct both from that of neuronal HSR induction and from other glial stress responses. This response is independent of the canonical *C. elegans* neuronal thermosensory circuit for HSR induction and of dense core vesicle release. It requires the presence of small clear vesicle release machinery, though no single neurotransmitter known to be released through these vesicles is independently required for the peripheral HSR induction. CEPsh glial *hsf-1* coordinates the upregulation of immune regulators, resulting in pathogen resistance. These data implicate *C. elegans* CEPsh glia as primary sensors and signalers of protein health insults, which can flexibly and specifically adopt signaling strategies to coordinate health and longevity across the organism.

Results:

To assess whether the four C. elegans CEPsh glia upregulate a protective HSR organismally in response to hsf-1, we created strains over-expressing hsf-1 under the CEPsh glia-specific promoter *hlh-17 (hlh-17p::hsf-1)* (17, 21, 22). To evaluate the impact of hlh-17p::hsf-1, CEPsh glial hsf-1, on longevity, we first assayed lifespan under normal culture conditions. We found that CEPsh glial *hsf-1* animals were longer lived than wild type N2 animals (Figure 1A, Supp Fig 1A). We also observed that this coincides with a suppression of fecundity (Supp Fig 1B, C). This is consistent with existing work suggesting increased HSF-1 function in lifespan is a trade-off with reproductive fitness (1, 23). This consequence may explain why hsf-1 expression is tightly titrated across evolution. However, we found that on the individual organism level, sterility was not correlated with lifespan extension, and non-sterile animals alongside sterile animals exhibited extension with glial *hsf-1* (Supp Fig 1D). We next examined heat stress tolerance and found that CEPsh glial *hsf-1* animals are robustly thermotolerant compared to wildtype N2 animals (Figure 1B, Supp Fig 1E). To test whether the increased longevity and stress tolerance of CEPsh glial *hsf-1* animals correlate with organismal induction of HSR genes, we used a fluorescent transcriptional reporter for *hsp-16.2*, a heat shock chaperone induced upon heat stress. Using this system, we found that CEPsh glial *hsf-1* animals strongly upregulated HSR chaperones upon heat stress compared to reporter animals alone, and that this increased expression was evident throughout the worm, predominantly visible in the intestine (Figure 1C and D, Supp Fig 1F, G). We also found that both the amphid sheath promotor fig-1 and the pan-glial, though somewhat non-specific promoter *mir-228* failed to induce such a response when over-expressing *hsf-1*, implying that there may be a dynamic interplay between multiple glial subtypes in which CEPsh glia are primarily activators of the HSR (Supp Fig 2A-C) (24). We thus determined that CEPsh glia non-autonomously induce the HSR, increasing longevity, stress response activation, and stress tolerance.

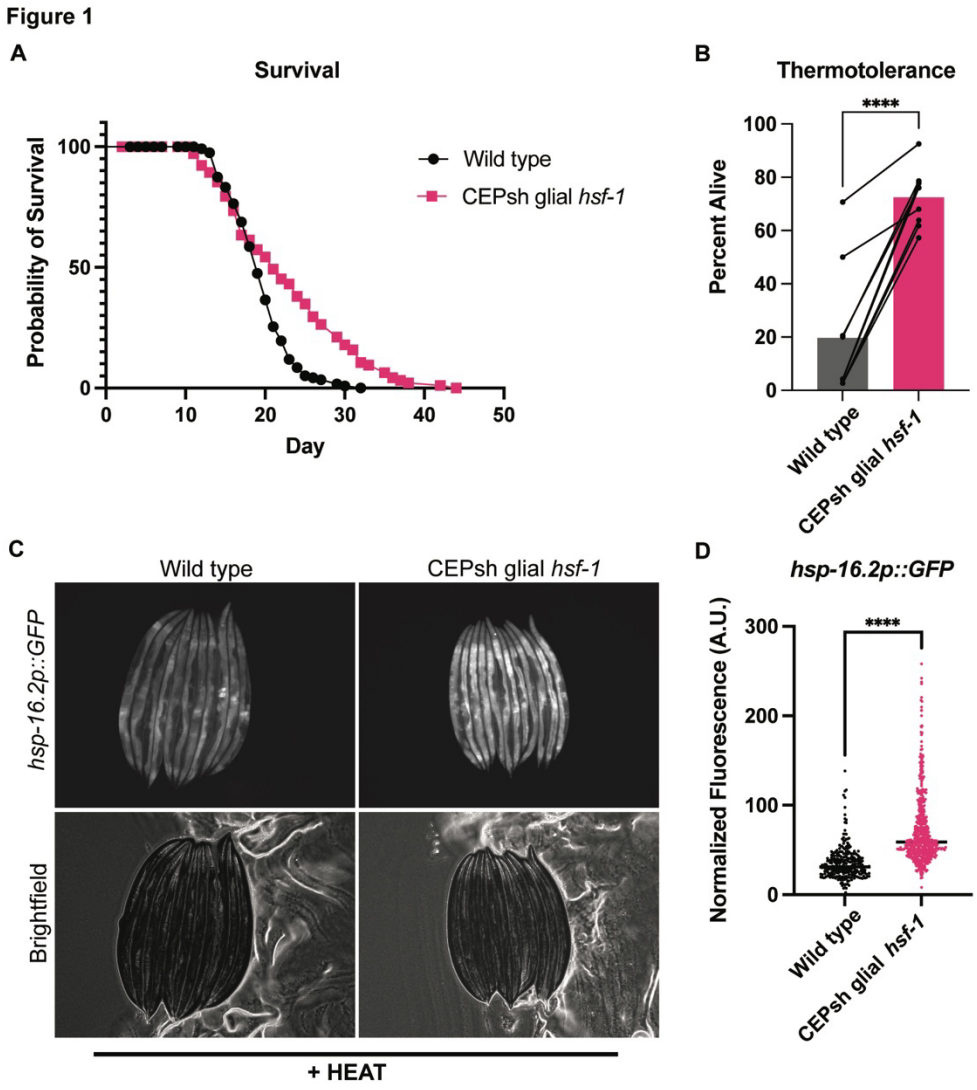

Figure 1: Over-expression of hsf-1 in CEPsh glia increases lifespan and stress tolerance by non-autonomously inducing the heat shock response. A) Survival of *hlh-17p::hsf-1* (integrated array) is significantly greater than wild type N2 at 20°C. Mean survival of N2 = 19 days, *Is1(hlh-17p::hsf-1)* = 21 days, p= 0.017. N=150 for each. B) Thermotolerance of *Ex(hlh-17p::hsf-1)* array expressing animals is significantly increased relative to wild type N2 animals after heat stress at 34°C for 12-16h. Connected points are individual experiments, p<0.0001. N=75 for each condition for each experiment C) *hsp-16.2p::GFP* transcriptional reporter worms with and without *Ex(hlh-17p::hsf-1)* after mild heat stress and recovery, lined up head to tail. D) Quantification of worm fluorescence strains in C in large particle flow cytometry via COPAS biosorter. *Ex(hlh-17p::hsf-1)* worms (N=507) are significantly brighter than *hsp-16.2p::GFP* alone (N=290), p < 0.0001. Representative experiment shown of >3 experiments.

Supplementary Figure 1

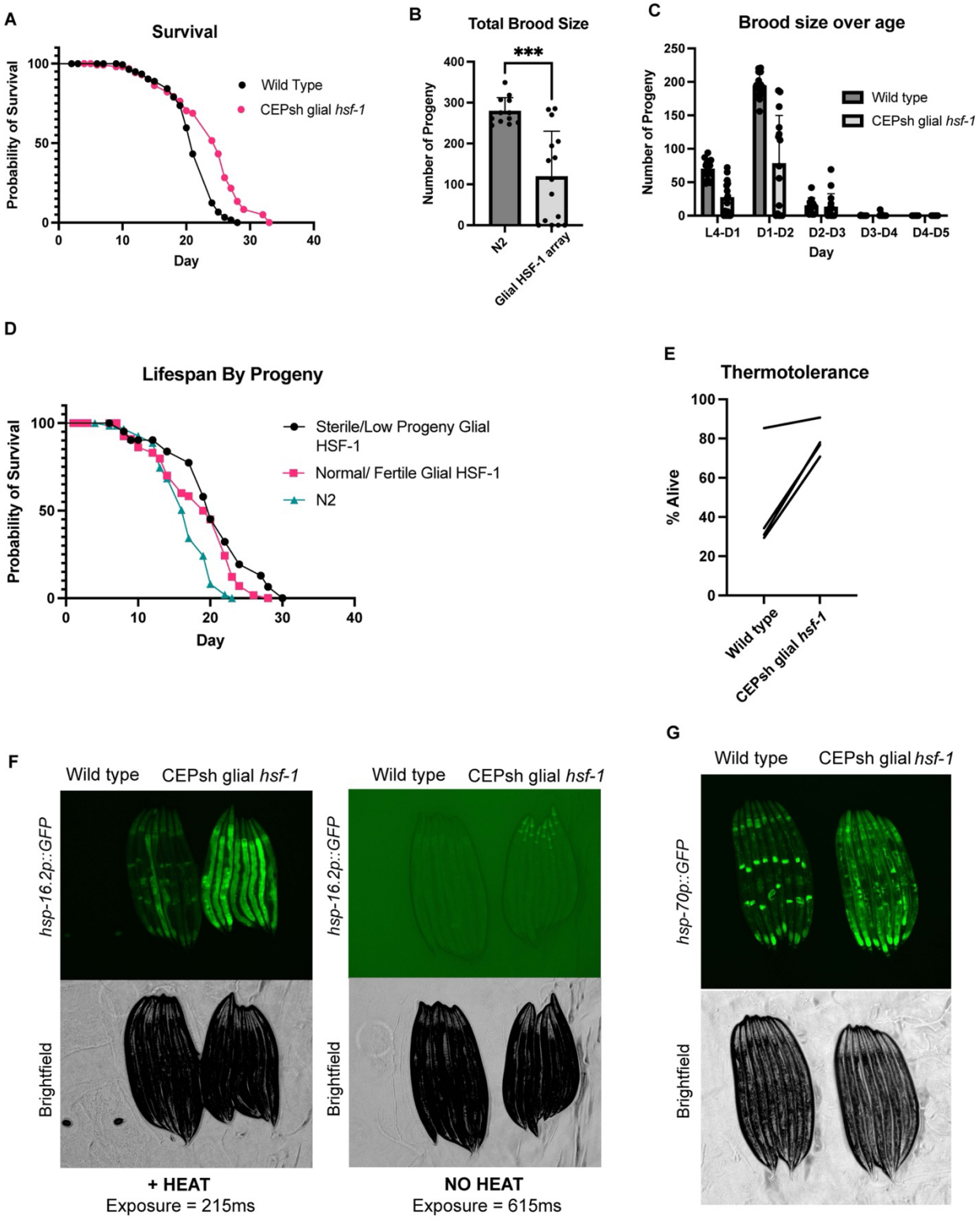

Supplementary Figure 1: Phenotype of CEPsh glial *hsf-1* and reproductive effects A) Lifespan of independent integrated array *Is2(hlh-17p::hsf-1)* is increased relative to wild type N2 animals. Median of N2 = 21 days, median of *Is2(hlh-17p::hsf-1)* = 25 days, $p < 0.001$. N= 150 for each condition B) Total brood size over the reproductive lifespan; *Ex(hlh-17p::hsf-1)* have significantly fewer progeny than wild type N2, $p < 0.001$. Error bars are SD, points are individual worms C) Brood size depicted across days of the reproductive lifespan. Error bars are SD, points are individual worms D) Lifespan of *Ex(hlh-17p::hsf-1)* versus wild-type worms segmented by individual worm sterility. N=150 per condition. E) Thermotolerance of independent integrated array *Is2(hlh-17p::hsf-1)* is increased relative to wild type N2 animals, p= 0.03. N=75 for each condition per experiment. F) *hsp-16.2p::GFP* transcriptional reporter worms *Is2(hlh-17p::hsf-1)* versus wild type N2 after mild heat stress and recovery (left) and basally without heat stress (right), lined up head to tail. Note that bleed-through from *myo-2p::tdtomato* is visible at increased exposure (right) G) *hsp-70p::GFP* transcriptional reporter worms *Is2(hlh-17p::hsf-1)* versus wild type N2 after mild heat stress and recovery, lined up head to tail.

Supplementary Figure 2

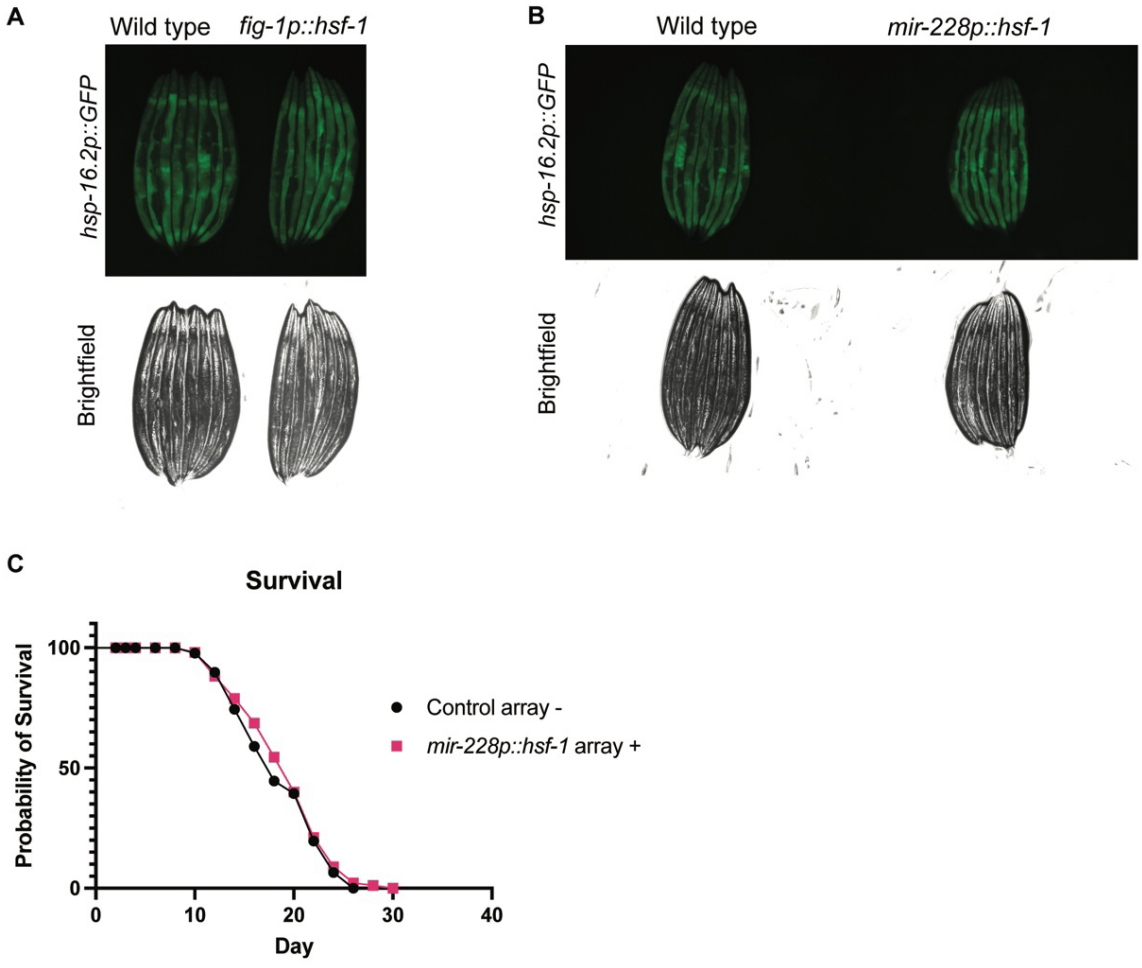

Supplementary Figure 2: Other glial subtype promoters are insufficient to activate a peripheral HSR A) *Ex(fig-1p::hsf-1); hsp-16.2p::GFP* animals (right) do not display consistent increase in fluorescence relative to *hsp-16.2p::GFP* alone (left) B) *Ex(mir-ww8p::hsf-1); hsp-16.2p::GFP* animals (right) do not display consistent increase in fluorescence relative to *hsp-16.2p::GFP* alone (left) C) Survival of *mir-228p::hsf-1* (extrachromosomal array) is not significantly increased relative to array negative animals at 20°C. N=150 worms for each condition.

Under natural heat sensing conditions, the AFD thermosensory neuron signals to the AIY interneuron, which is upstream of serotonergic neurons such as NSM and ADF (Figure 2A) (*18*, *58*). To ascertain whether the heat stress response to glial *hsf-1* is mediated by the canonical thermosensory neuronal circuitry for HSR induction, we measured induction of *hsp-16.*2 in mutants defective in AIY interneuron formation, *ttx-3(ks5)*, with CEPsh glial *hsf-1* over-expression. *ttx-3(ks5)* mutants have been previously shown to decrease induction of the HSR in otherwise wild type animals (*17*). We found that under acute heat shock, *ttx-3(ks5)* mutant animals with CEPsh glial *hsf-1* still exhibited increased levels of *hsp-16.2* relative to *ttx-3(ks5)* mutants alone (Figure 2B, C). We thus determined that the AIY interneuron is not wholly required for the non-cell autonomous signaling from CEPsh glia due to *hsf-1* over-expression. Unexpectedly, we also found that under this acute heat shock protocol, *ttx-3(ks5)* mutants may exhibit higher levels of *hsp-16.2p::GFP* relative to wild type animals, although we did not consistently observe a significant increase by COPAS biosorter quantification across replicates. Taken together, these data suggest that the contribution of glia to HSR induction may be either downstream of or independent of AIY thermosensory neuron function, unlike the neuronal HSR.

Due to the apparent divergence of glial HSR regulation from this thermosensory circuit component, we next asked whether other members of the core HSR induction circuitry were dispensable for CEPsh glial *hsf-1* signaling. Serotonin and serotonin receptor activity are also required for downstream sensing of the AFD/AIY thermosensory circuit and HSR induction (*18*). Therefore, we next examined animals with the *tph-1(mg280)* mutation, which lack functional tryptophan hydroxylase and are unable to synthesize serotonin, for induction of *hsp-16.2* by CEPsh glial *hsf-1*. We found that serotonin synthesis is dispensable for peripheral induction of *hsp-16.2* by CEPsh glial *hsf-1*, implying that glial HSR induction is independent of serotonin (Figure 2D, E). To further examine the role of serotonin, we subjected CEPsh glial *hsf-1* animals with and without the *tph-1(mg280)* mutation to chronic heat stress. We found that serotonin synthesis is not required for the glial *hsf-1*-mediated increase in thermotolerance (Figure 2F). Unexpectedly, we also found that *tph-1(mg280)* animals may exhibit higher levels of *hsp-16.2p::GFP* and increased thermotolerance relative to wild type animals in these assays. Taken together, the signaling of the HSR by CEPsh glia does not occur via the canonical neuronal heat stress pathway, nor does it require serotonin.

Figure 2

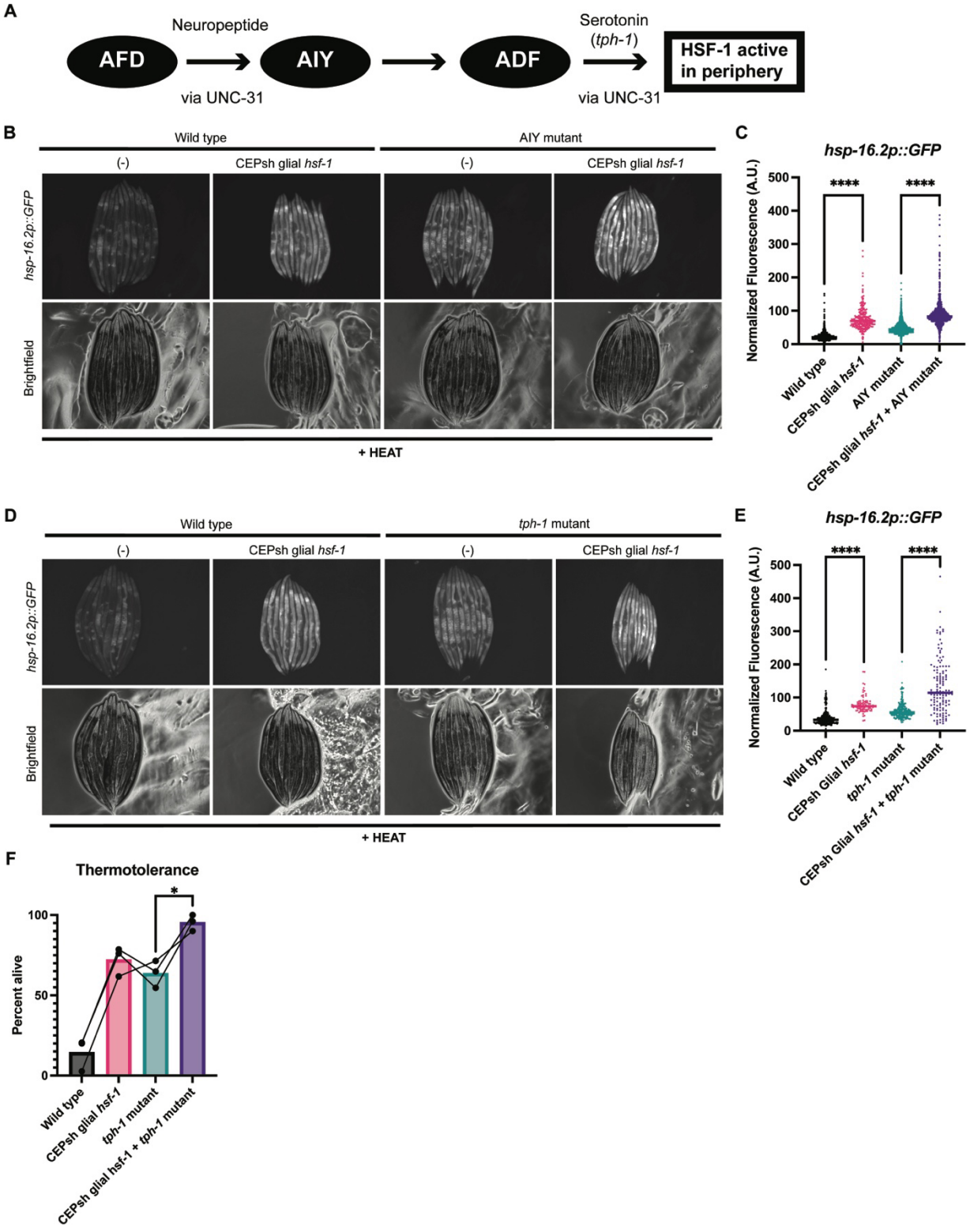
A
Neuropeptide
AFD
AIY
ADF
Serotonin
(tph-1)
HSF-1 active
in periphery
via UNC-31
via UNC-31
B
Wild type
AIY mutant
(-)
CEPsh glial hsf-1
(-)
CEPsh glial hsf-1
hsp-16.2p::GFP
Brightfield
+ HEAT
C
hsp-16.2p::GFP
Normalized Fluorescence (A.U.)
****
****
Wild type
CEPsh glial hsf-1
AIY mutant
CEPsh glial hsf-1 + AIY mutant
D
Wild type
tph-1 mutant
(-)
CEPsh glial hsf-1
(-)
CEPsh glial hsf-1
hsp-16.2p::GFP
Brightfield
+ HEAT
E
hsp-16.2p::GFP
Normalized Fluorescence (A.U.)
****
****
Wild type
CEPsh Glial hsf-1
tph-1 mutant
CEPsh Glial hsf-1 + tph-1 mutant
F
Thermotolerance
*
Percent alive
Wild type
CEPsh glial hsf-1
tph-1 mutant
CEPsh glial hsf-1 + tph-1 mutant

Figure 2: The canonical thermosensory HSR circuit is dispensable for CEPsh glial *hsf-1* signaling. A) Schematic of the thermosensory circuit and relevant signaling components. B) Mutants for AIY, *ttx-3(ks5)*, with and without *Ex(hlh-17p::hsf-1)* imaged for the *hsp-16.2p::GFP* after mild heat stress and recovery. *Ex(hlh-17p::hsf-1); ttx-3(ks5)* exhibit higher *hsp-16.2p::GFP* fluorescence than *ttx-3(ks5)* alone. C) Quantification of strains in B via large particle flow cytometry. *Ex(hlh-17p::hsf-1); ttx-3(ks5)* are brighter than *ttx-3(ks5)* alone ($p < 0.0001$). Wild type N=1014, CEPsh glial *hsf-1* N= 253, *ttx-3* N=2767, CEPsh glial *hsf-1* + *ttx-3* N= 1171. Representative experiment shown of 3 experiments. D) Mutants for tryptophan hydroxylase, *tph-1(mg280)*, with and without *Ex(hlh-17p::hsf-1)* imaged for the *hsp-16.2p::GFP* after mild heat stress and recovery. *Ex(hlh-17p::hsf-1); tph-1(mg280)* animals exhibit higher *hsp-16.2p::GFP* fluorescence than *tph-1(mg280)* animals alone. E) Quantification of strains in D via large particle flow cytometry. *Ex(hlh-17p::hsf-1); tph-1(mg280)* animals are significantly brighter than *tph-1(mg280)* alone ($p < 0.0001$). Wild type N=263, CEPsh glial *hsf-1* N=87, *tph-1* N=239, CEPsh glial *hsf-1* + *tph-1* N=131. Representative experiment shown of 3 experiments. F) Thermotolerance of wild type N2 animals, *Ex(hlh-17p::hsf-1)* animals, *tph-1(mg280)* animals, and *Ex(hlh-17p::hsf-1); tph-1(mg280)*. Data points are individual experiments, and connecting line indicates paired trials. Error bars are S.D. Thermotolerance of *Ex(hlh-17p::hsf-1); tph-1(mg280)* is significantly greater than *tph-1(mg280)* ($p=0.04$). N=75 for each condition for each experiment.

We next asked which signaling molecules might be responsible for this non-cell autonomous signaling of the HSR to peripheral tissues by CEPsh glia, if not serotonin. Previous studies of stress signaling from glia in the case of the ER and mitochondrial UPRs implicated neuropeptides (*26*, *51*). CEPsh glia could regulate distinct stress responses with similar or distinct signals. Dense core vesicles are required for the release of larger cargos, like neuropeptides, while small clear vesicles are required for neurotransmitter release (*59*, *60*). To determine whether small clear vesicles or dense core vesicles might be required for non-cell autonomous HSR induction in CEPsh glial *hsf-1* animals, we used mutants for the vesicular release components *unc-13* and *unc-31*, respectively (*59*, *60*). We found that loss of small clear vesicle fusion via *unc-13(s69)* suppressed CEPsh glial *hsf-1* non-cell autonomous induction of *hsp-16.2* (Figure 3A, B). In contrast, loss of dense core vesicle fusion via *unc-31(e958)* mutation failed to completely suppress the increase in peripheral *hsp-16.2* activation (Figure 3C, D) (*59*, *60*). Taken together, these data indicate that CEPsh glial signaling of the HSR relies on cargo enclosed in small clear vesicles and is independent of dense core vesicle neuropeptide signaling, unlike the neuronal and glial mitochondrial UPR and glial UPR ER responses (*26*, *51*).

As the canonical cargoes for small clear vesicles in the worm are neurotransmitters, we selected a set of mutants in synthesis or vesicular loading for each of the known neurotransmitters in *C. elegans*. Having already assessed serotonin, we turned our attention to mutants defective in signaling by glutamate (*eat-4*), GABA (*unc-25*), dopamine (*cat-2*), acetylcholine (*unc-17*), and octopamine and tyramine (*tdc-1*). Using the thermotolerance assay, we found that the increase in survival due to CEPsh glial *hsf-1* is preserved in the absence of dopamine, GABA, and octopamine/tyramine (Figure 3E, Supp. Figure 3). Further, there is a trend towards significance in the survival increase of acetylcholine and glutamate mutants (Figure 3E, Supp. Figure 3). Notably, acetylcholine and glutamate are canonical small clear

vesicle cargoes, though the apparent partial suppression of effect suggests neither transmitter is independently required for signaling (Supp. Figure 3D, E). These data suggest that no known neurotransmitter is independently responsible for organismal protection against heat stress conferred by CEPsh glial *hsf-1*, though the signal is likely contained in an UNC-13-mediated vesicle.

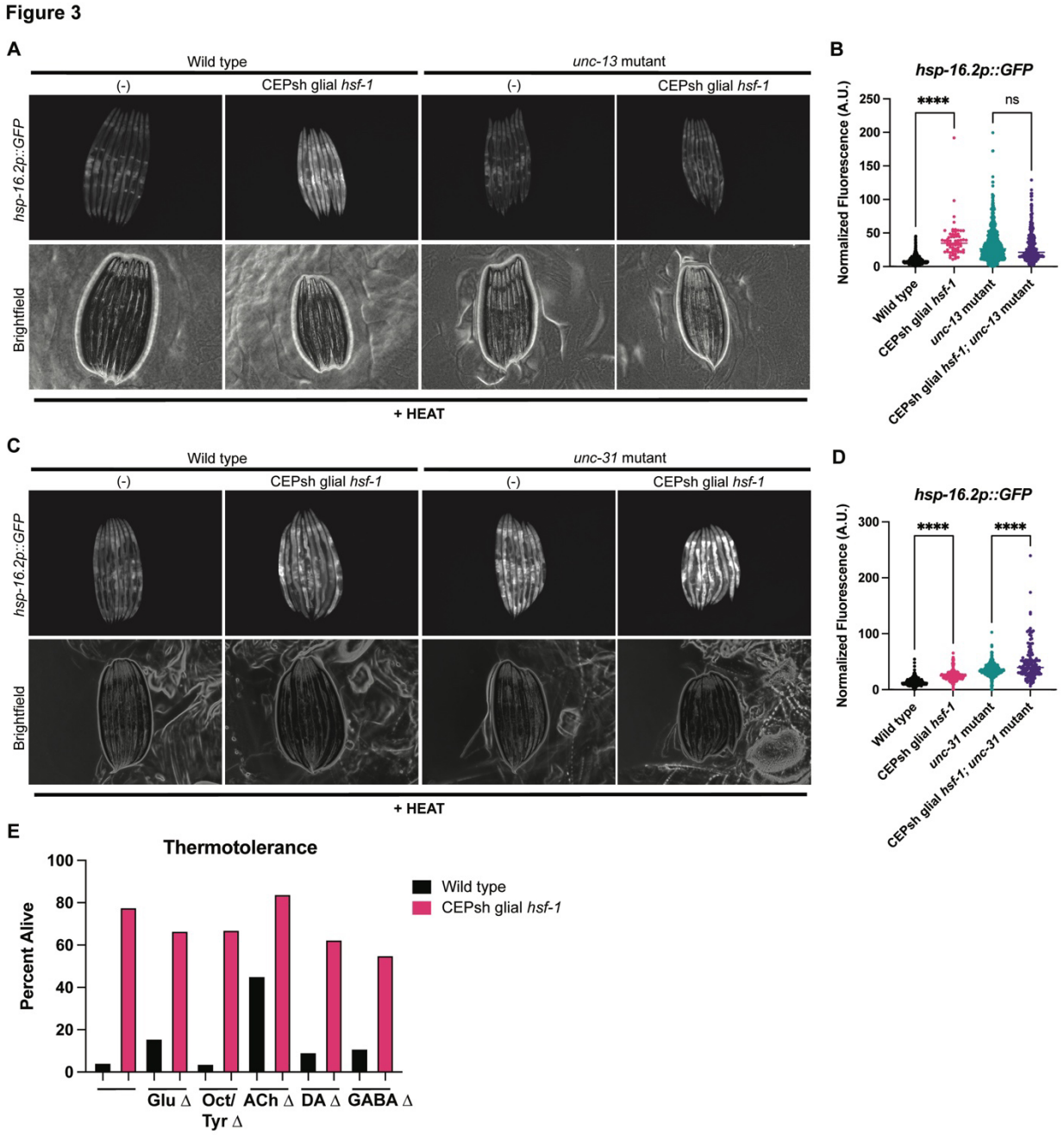

Figure 3: Small clear vesicles, but not dense core vesicles, are required for CEPsh glial *hsf-1* signaling via an unknown cargo. A) Mutants for small clear vesicle release, *unc-13(s69)*, with and without *Ex(hlh-17p::hsf-1)* imaged for *hsp-16.2p::GFP* after mild heat stress and recovery.

Unc-13(s69), *Ex(hlh-17p::hsf-1)* animals have no increase in *hsp-16.2p::GFP*. B) Quantification of strains in A via large particle flow cytometry. Fluorescence of *Ex(hlh-17p::hsf-1); unc-13(s69); hsp-16.2p::GFP* animals is not significantly increased vs. *unc-13(s69); hsp-16.2p::GFP*. Wild type N=548, CEPsh glial *hsf-1* N=67, *unc-13* N=1000, CEPsh glial *hsf-1 + unc-13* N=304. Representative experiment shown of 3 experiments. C) Mutants for dense core vesicle release, *unc-31(e958)*, with and without *Ex(hlh-17p::hsf-1)* imaged for the reporter *hsp-16.2p::GFP* after mild heat stress and recovery. *Unc-31(e958)*, *Ex(hlh-17p::hsf-1)* animals exhibit an increase in *hsp-16.2p::GFP*. D) Quantification of strains in C via large particle flow cytometry. Fluorescence of *Ex(hlh-17p::hsf-1); unc-31(se958); hsp-16.2p::GFP* animals is significantly increased relative to *unc-31(e958); hsp-16.2p::GFP* ($p<0.0001$). Wild type N=559, CEPsh glial *hsf-1* N=166, *unc-31* N=535, CEPsh glial *hsf-1 + unc-31* N=140. Representative experiment shown of 3 experiments. E) Thermotolerance of *Ex(hlh-17p::hsf-1)* (pink) and wild type N2 (black) animals. Neurotransmitter mutation is on the x axis, such that the left-most comparison of *Ex(hlh-17p::hsf-1)* and wild type N2 is in the wild type background, followed by Glu = *eat-4(ky5)*, Oct/Tyr = *tdc-1(n3419)*, ACh = *unc-17(e245)*, DA = *cat-2(n4547)*, GABA = *unc-25(e156)*. Representative experiment displayed, with at least 3 replicates for each mutant condition, less *unc-25* with 2 replicates.

Supplementary Figure 3

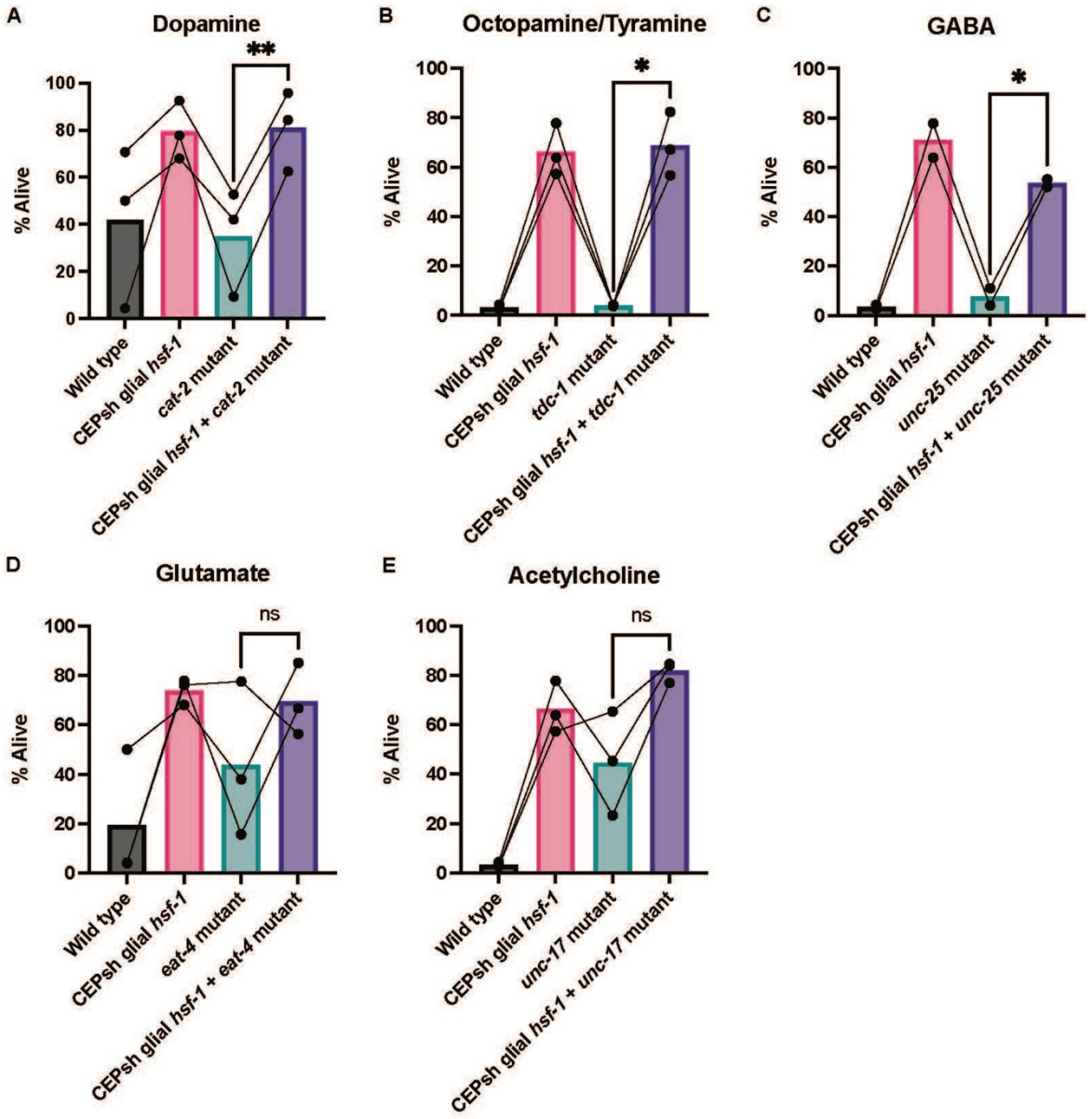

Supplementary Figure 3: Thermotolerance of neurotransmitter mutants. Mutants for each neurotransmitter alone are displayed in blue, and CEPsh glial *hsf-1* with the relevant neurotransmitter mutant is displayed in purple. For each, N=75 animals per condition per experiment, statistically N=3 experiments. Each point is an experiment. A) Thermotolerance of *Ex(hlh-17p::hsf-1); cat-2(n4547)* is significantly increased relative to *cat-2(n4547)* alone, p= 0.03. B) Thermotolerance of *Ex(hlh-17p::hsf-1); tdc-1(n3419)* is significantly increased relative to *tdc-1(n3419)* alone, p= 0.04. C) Thermotolerance of *Ex(hlh-17p::hsf-1); unc-25(e156)* is significantly increased relative to *unc-25(e156)* alone, p=0.02. D) Thermotolerance of *Ex(hlh-17p::hsf-1); eat-4(ky5)* is not significantly increased relative to *eat-4(ky5)* alone, though there is a trend towards increase. E) Thermotolerance of *Ex(hlh-17p::hsf-1); unc-17(e245)* is not significantly increased relative to *unc-17(e245)* alone, though there is a trend towards increase.

Neuronal HSR signaling relies on both HSF-1 and the insulin signaling-related FOXO homolog DAF-16 in peripheral tissues to enact survival benefits. Therefore, we tested the requirement for these transcription factors in peripheral HSR activation of CEPsh glial *hsf-1* animals (*5*). Neurons and CEPsh glia of *C. elegans* are partially resistant to RNA interference (RNAi), allowing us to interrogate peripheral signaling requirements (Supp. Figure 4A) (*61*). Examining induction of the *hsp-16.2* transcriptional reporter, we found that, as predicted, *hsf-1* is required in peripheral cells for most HSR chaperone induction (Figure 4A, B). In contrast, *daf-16* is not required for peripheral *hsp-16.2* induction, although we sometimes observed a small overall reduction in level of *hsp-16.2* (Figure 4C, D). Despite these differences in chaperone induction, the increase in lifespan due to CEPsh glial *hsf-1* was largely dependent on both *hsf-1* and *daf-16* in peripheral tissues (Figure 4E-F). Further, *hsf-1* and *daf-16* seem to be at least partially required for thermotolerance increase (Supp. Figure 5B, C). Overall, these data indicate that *hsf-1* and *daf-16* act in concert to regulate the protective phenotypes of CEPsh glial *hsf-1* animals in the peripheral tissues.

Supplementary Figure 4

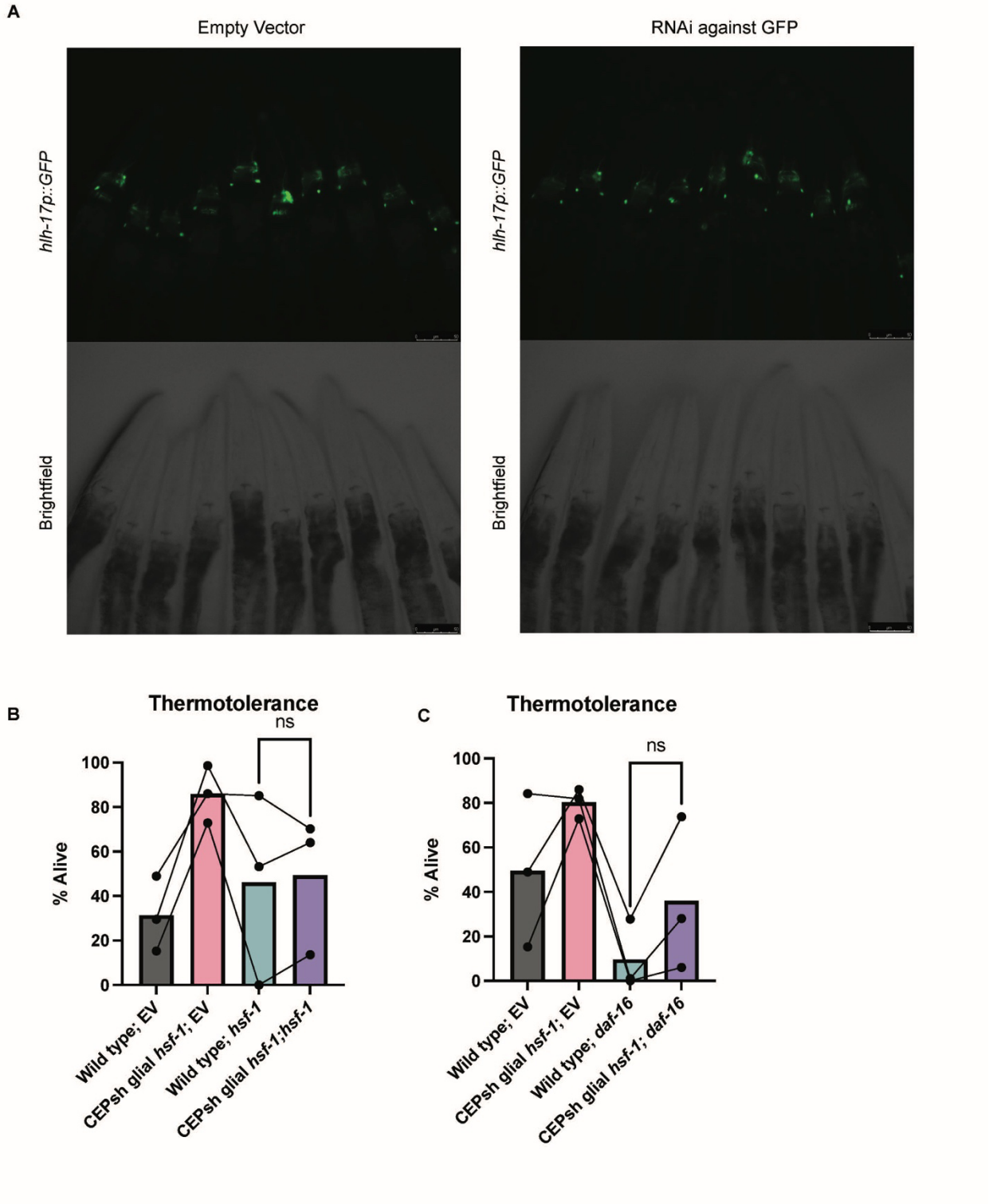

Supplementary Figure 4: Effects of RNAis on CEPsh glia A) CEPsh glial GFP via *hlh-17p::GFP* is not knocked down when exposed to RNAi against GFP (right), as compared to signal on empty vector bacteria (left) B) Thermotolerance of *Ex(hlh-17p::hsf-1)* eating *hsf-1* RNAi

bacteria (blue) is not significantly increased relative to that of wild type N2 worms eating *hsf-1* RNAi (purple). For each, N=75 animals per condition per experiment, statistically N=3 experiments. C) Thermotolerance of *Ex(hlh-17p::hsf-1)* eating *daf-16* RNAi bacteria (blue) is not significantly increased relative to that of wild type N2 worms eating *daf-16* RNAi (purple). For each, N=75 animals per condition per experiment, statistically N=3 experiments.

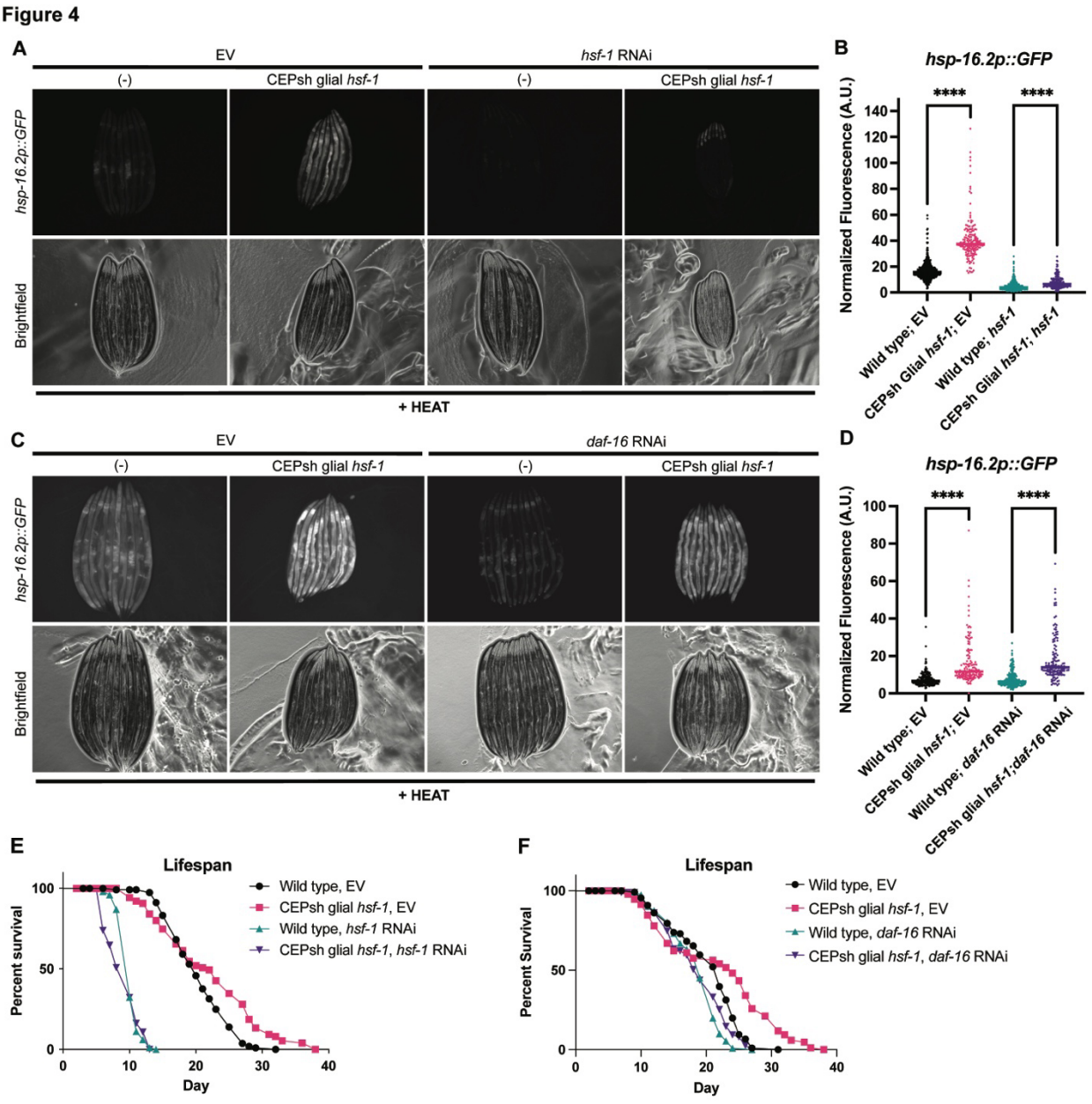

Figure 4: HSF-1 and DAF-16 are required for benefits of CEPsh glial *hsf-1* in peripheral tissues. A) Wild type and *Ex(hlh-17p::hsf-1)* imaged for the reporter *hsp-16.2p::GFP* after mild heat stress and recovery under empty vector (EV) and *hsf-1* RNAi conditions. RNAi against *hsf-1*

suppresses *hsp-16.2p::GFP*. B) Quantification of strains in A via large particle flow cytometry. *Ex(hlh-17p::hsf-1)*-related *hsp-16.2p::GFP* induction is partially suppressed by *hsf-1* RNAi, though *Ex(hlh-17p::hsf-1)* on *hsf-1* RNAi remains significantly increased vs. wild type N2 on *hsf-1* RNAi ($p<0.0001$). Wild type on EV N=568, CEPsh glial *hsf-1* on EV N=169, Wild type on *hsf-1* N=707, CEPsh glial *hsf-1* on *hsf-1* N=200. Representative experiment shown of 3 experiments. C) Wild type and *Ex(hlh-17p::hsf-1)* imaged for *hsp-16.2p::GFP* after mild heat stress and recovery on EV and *daf-16* RNAi. D) Quantification of strains in C via large particle flow cytometry. *Ex(hlh-17p::hsf-1)* on *daf-16* RNAi remains significantly increased vs. wild type N2 animals on *daf-16* RNAi ($p<0.0001$). Wild type on EV N=165, CEPsh glial *hsf-1* on EV N=158, Wild type on *daf-16* N=272, CEPsh glial *hsf-1* on *daf-16* N=139. Representative experiment shown of 3 experiments. E) Lifespan of *Is1(hlh-17p::hsf-1)* vs. wild type N2 worms on EV and *hsf-1* bacteria. Mean survival of N2 on EV = 20 days, *Is1(hlh-17p::hsf-1)* on EV = 22 days, N2 on *hsf-1* RNAi = 10 days, and *Is1(hlh-17p::hsf-1)* on *hsf-1* RNAi = 10 days, $p<0.0001$. N=150 animals per experiment. F) Lifespan of *Is1(hlh-17p::hsf-1)* vs. wild type N2 worms on EV and *daf-16* bacteria. Mean survival of N2 on EV = 22 days, *Is1(hlh-17p::hsf-1)* on EV = 24 days, N2 on *daf-16* RNAi = 19 days, and *Is1(hlh-17p::hsf-1)* on *daf-16* RNAi = 19 days, $p= 0.0012$. N=150 animals per experiment.

Beyond known HSR effectors, we next sought to identify organismal changes in gene expression that might shed light on peripheral tissues' interpretation of glial *hsf-1* signaling. Whole animal RNA sequencing (RNA-seq) revealed substantial gene expression changes in CEPsh glial *hsf-1* animals compared to wild type N2 animals, with 692 genes significantly upregulated and 272 genes downregulated (adj-p <= .05 and log2(FC) of greater than 1 or less than -1, respectively). In CEPsh glial *hsf-1* animals, *hsf-1* is significantly upregulated, and HSR genes *hsp-16.2* and *hsp-70* are mildly increased, while chaperones for the ER and mitochondrial UPRs were either unchanged or downregulated, respectively (Figure 5A). We further validated these transcriptional changes by use of a fluorescent reporter for *gst-4*, a gene which exhibited a mild increase in expression in our dataset and by reporter imaging (Supp. Figure 5). To identify high confidence HSF-1-regulated genes that were differentially expressed in the CEPsh glial *hsf-1* animals, we generated a list of genes that were previously reported to be HSF-1 targets and had HSF-1 binding sites in the immediate upstream region from the start codon (*62*). Indeed, many high confidence HSF-1 target genes were significantly upregulated or downregulated ($p<0.05$) in CEPsh glial *hsf-1* animals (Figure 5B). Interestingly, these data imply that HSF-1 may be activating as both a transcriptional activator and repressor, as others have previously indicated (*62–64*). To evaluate the categories in which whole animal gene expression was altered by sensing CEPsh glial *hsf-1*, we used gene ontology (GO) analysis of upregulated and downregulated genes (*65*, *66*). GO term enrichment analysis of the significantly upregulated genes contained GO terms concerning the immune response and stress responses generally, while GO terms associated with the significantly downregulated genes highlighted protein modification (Figure 5C). Overall, sequencing analysis of the CEPsh glial *hsf-1* animals reveals a broad upregulation of immune and stress response genes with differential expression of many *bona fide* HSF-1 target genes.

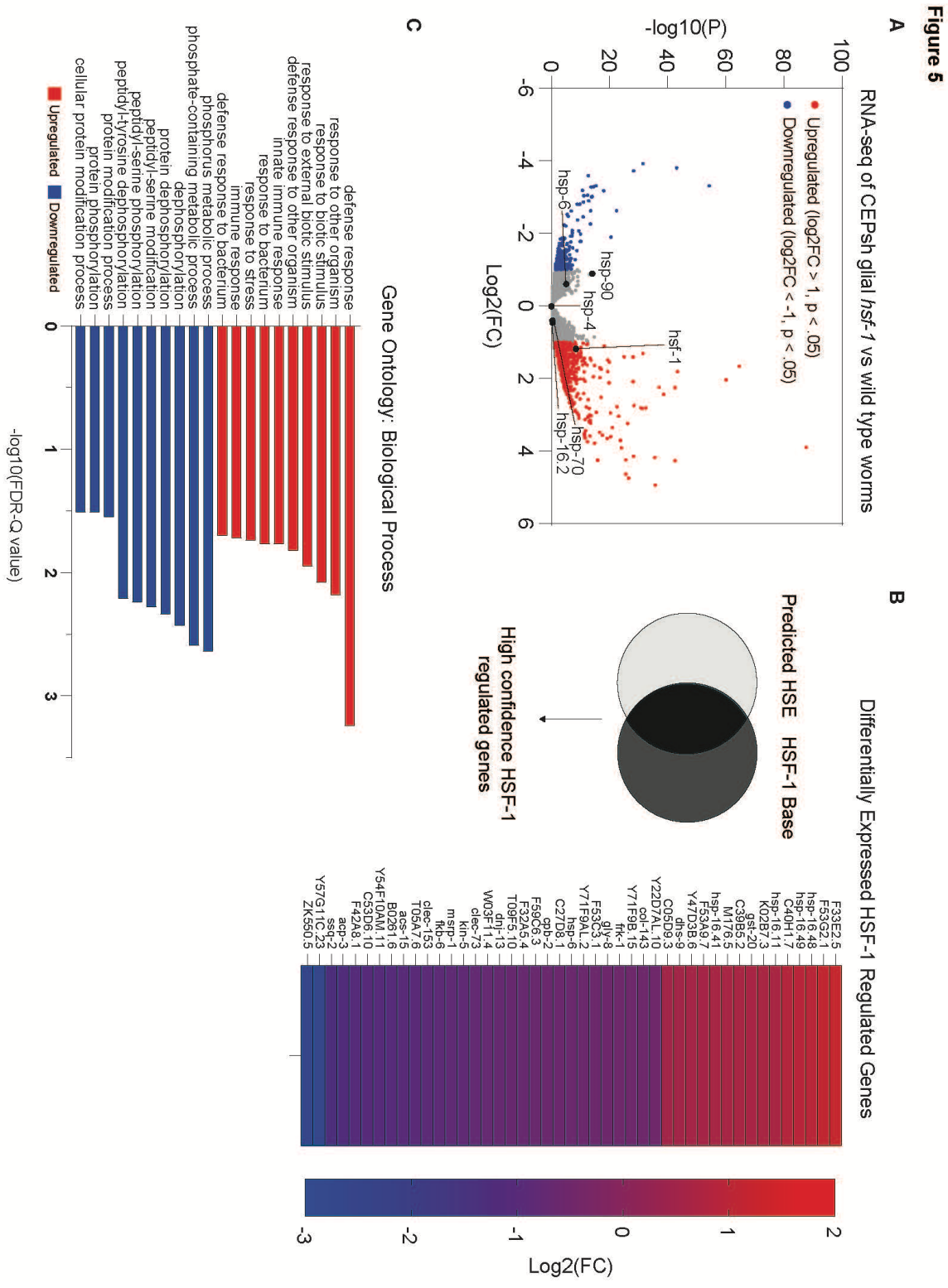

Figure 5: CEPsh glial *hsf-1* induces peripheral changes in HSF-1-regulated genes and the immune response. A) Volcano plot demonstrating magnitude (Log2(FC)) and significance (-log10(p-value)) of changes in gene expression from whole-animal RNA sequencing of *Is1(hlh-*

17p::hsf-1) versus wild type N2. Labeled genes are stress genes, including *hsf-1* and HSR chaperones *hsp-70*, *hsp-16.2* (HSF-1 regulated) and *hsp-90* (non-HSF-1 regulated), as well as ER UPR chaperone *hsp-4* and mitochondrial UPR chaperone *hsp-6*. B) High confidence HSF-1-regulated genes are displayed alongside their Log2(FC) values, color coded from cool (down-regulated) to warm (up-regulated). C) The top ten Gene Ontology (GO) terms for up- (red) and down- (blue) regulated genes are displayed with their -log10 corrected FDR-Q value.

Supplementary Figure 5

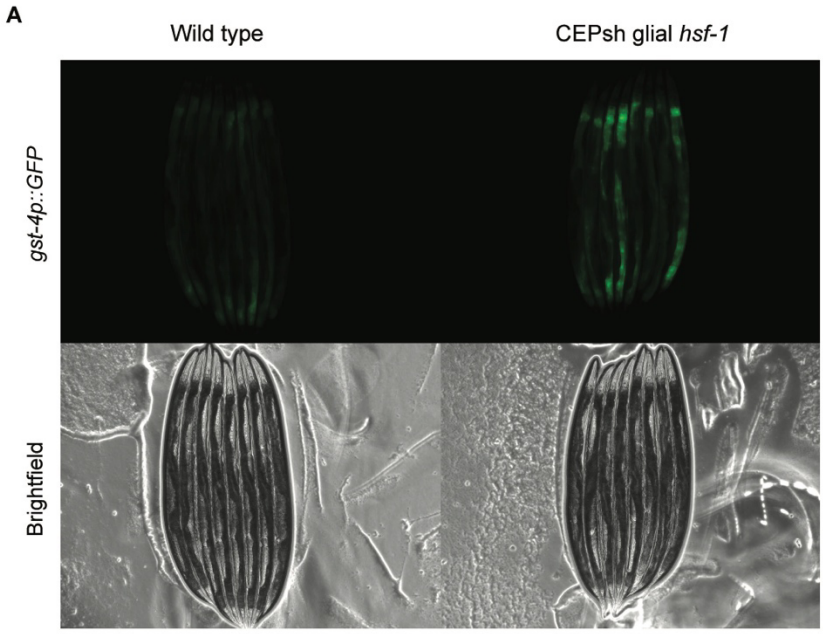

Supplementary Figure 5: Validation of RNA sequencing by transcriptional reporter A) CEPsh glial *hsf-1* animals display increased *gst-4p::GFP* relative to wild type animals.

Infectious insults are important natural environmental stimuli for worms, and infection is a major cause of death across the organism's lifespan (*67*). The bacteria *Pseudomonas aeruginosa* is pathogenic to *C. elegans*, and *hsf-1* is required for normal survival on *P. aeruginosa* (*68*). Further, heat shock chaperones are activated upon exposure to the bacteria (*57*). Given data suggesting a broad upregulation of immune genes in CEPsh glial *hsf-1* animals, we hypothesized that CEPsh glial *hsf-1* might induce a pathogen resistance program. We first evaluated whether chaperone induction or lifespan of CEPsh glial *hsf-1* animals were dependent on canonical immune regulators *pmk-1* and *skn-1*. We found that each of the two factors were dispensable for peripheral chaperone induction (Supp Fig 6A) and lifespan, *skn-1* fully and *pmk-1* partially (Supp Fig 6B), implying that a non-canonical pathway may be activated. This would be consistent with previous works suggesting that *hsf-1* increases pathogen resistance by a non-canonical mechanism(*68*). Accordingly, we found no increase in an immune response fluorescent reporter downstream of *pmk-1* (Supp Fig 6C). We therefore tested resistance of CEPsh glial *hsf-1* versus wild type N2 worms on the *P. aeruginosa* PA14 strain using the slow

killing assay and found a robust increase in survival in CEPsh glial *hsf-1* animals (Figure 6A). However, we did not identify a deficit in survival on PA14 for worms expressing a caspase under the *hlh*-17 promoter, implying that pathogen survival does not exclusively rely on CEPsh glia (Supp. Fig 6D). These data suggest that CEPsh glial upregulation of HSF-1 activity drives a *bona fide*, HSF-1-regulated immune response that protects the animals from bacterial infection.

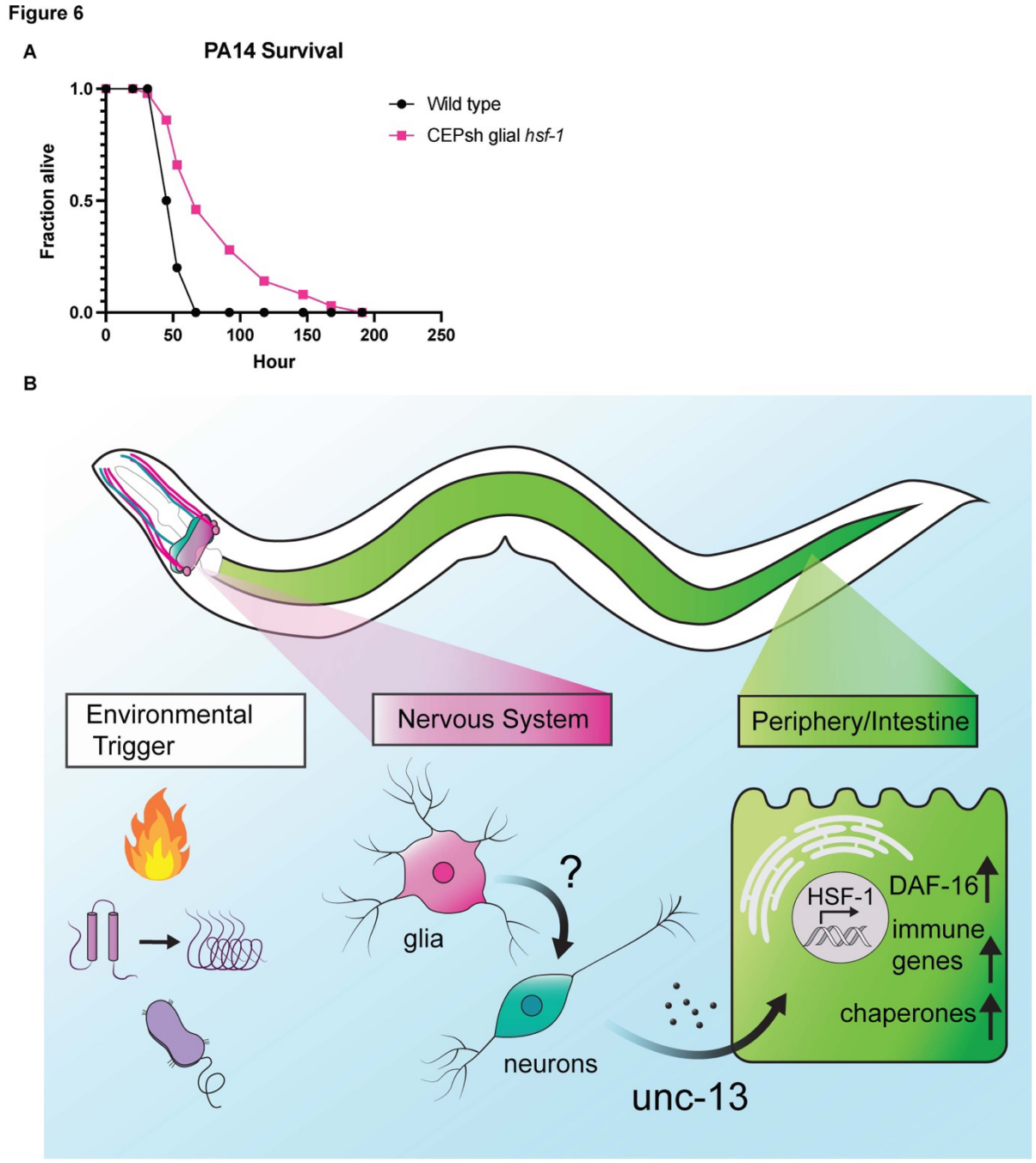

Figure 6: CEPsh glial *hsf-1* induces immune resistance. A) Survival of *Ex(hlh-17p::hsf-1)* is increased versus wild type N2 animals on *Pseudomonas aeruginosa* bacteria. Mean survival for

wild type N2 animals = 53h, for *Ex(hlh-17p::hsf-1)* animals = 67h. $p < 0.0001$ N=120 per condition B) Schematic summarizing findings. Heat, immune challenge, or misfolded proteins may activate signaling. Glial activation of *hsf-1* likely signals to neurons, causing release of some *unc-13*-dependent cue to peripheral cells. Downstream cells activate HSF-1 and DAF-16 as well as immune factors, to increase lifespan, stress tolerance, and immune resistance.

Supplementary Figure 6

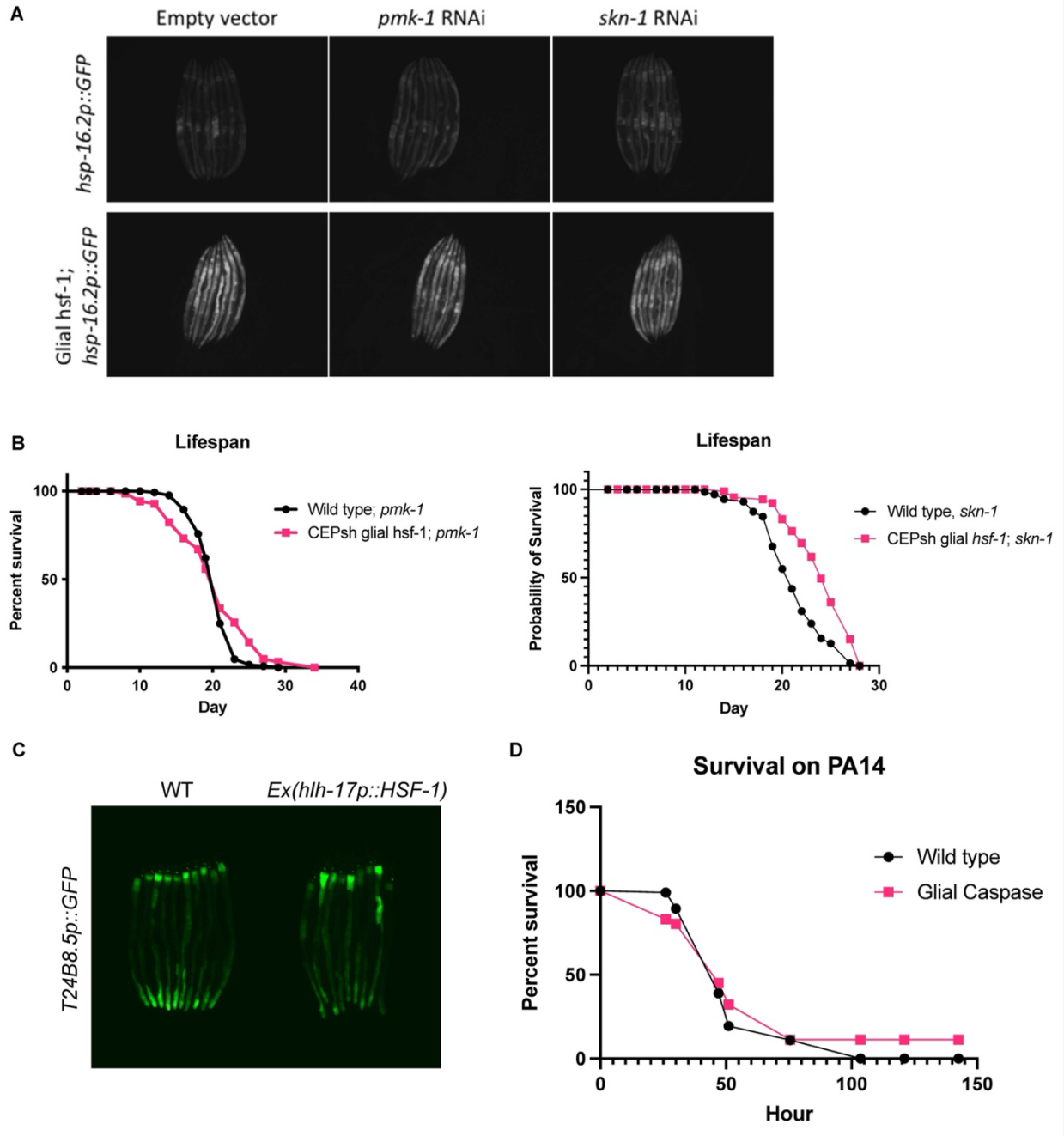

Supplementary Figure 6: CEPsh glial *hsf-1* phenotypes are independent of *skn-1*, *pmk-1* A) RNAi against *pmk-1* and *skn-1* fails to knock down peripheral induction of *hsp-16.2p::GFP* in *Ex(hlh-17p::hsf-1)* worms relative to wild-type N2 worms. B) Lifespans of *Is1(hlh-17p::hsf-1)* worms remain extended relative to wild-type N2 worms, primarily at the end of life, when *pmk-1* (left) or *skn-1* (right) are knocked down via RNAi. *Skn*-1 is statistically significant, $p<0.01$, *pmk-1* n.s. but retains end of life tail. N=150 per condition. C) The *T24B8.5p::GFP* reporter is not upregulated in *Ex(hlh-17p::hsf-1)* worms relative to wild-type N2 worms. D) Glial caspase animals are not short-lived relative to wild type animals on PA14. N=120 per condition.

Discussion:

We have identified a unique role for the four astrocyte-like CEPsh glia of *C. elegans* in coordinating a non-cell autonomous heat shock response. Animals over-expressing *hsf-1* in CEPsh glia are both more tolerant to heat stress and longer-lived. These phenotypes correlate with an increase in HSR chaperones across the animal, demonstrating the ability of CEPsh cells to induce the stress response in distal tissues by a diffuse signaling mechanism (Figure 6B). *C. elegans* have 959 somatic cells, 302 neurons, and 56 glia, among which only four are CEPsh glia. Previous work demonstrated beneficial effects on longevity when over-expressing *hsf-1* in all 302 neurons, which amount to nearly one third of the animal's cells; in this study, however, we over-express *hsf-1* in fewer than 0.5% of all cells of the worm and find similar effects on lifespan and stress tolerance (*5*). These data suggest that the worm is particularly responsive to stress signaling from CEPsh glia. As glia are best known for their interactions with neurons, it also suggests that glial stress responses may play a larger role in regulating neuronal stress response activity.

Interestingly, we show here that glial coordination of the HSR is independent of known components of the canonical thermosensory circuit for HSR induction. The AIY interneuron has been previously identified as a hub for integrating heat sensing (*5*, *17*); however, we find that this neuron is not required for non-cell autonomous signaling of the CEPsh glial HSR. Our identification of an UNC-13-dependent, non-AIY mediated glial signal for regulating lifespan via *hsf-1* signaling implies that two distinct pathways may be at work: one composed of thermosensory neuron components, and the other downstream of CEPsh glia. This is further evident in the independence of glial HSR signaling from serotonin, a downstream component of the thermosensory circuit. The existence of two such pathways may explain the surprising result that worms deficient in either AIY function or serotonin synthesis show a slight increase in heat shock chaperones upon acute heat shock relative to wild type animals by reporter imaging in our hands. Lack of canonical signaling in the case of these mutants may cause compensatory upregulation of the alternative pathway as a result, potentially via the CEPsh glia. Further work is needed to decipher the interaction between these systems.

Notably, the serotonin-independent nature of the CEPsh glial HSR mechanism differentiates it not only from the neuronal circuit controlling the HSR, but also from all other known neuronally-controlled proteostatic responses. Neurons ostensibly converge to regulate protein homeostasis using serotonin, which has been previously implicated in neuronal regulation of stress resistance via the HSR (*18*), the mitochondrial UPR (*35*), and the endoplasmic reticulum UPR (*34*). The CEPsh glial HSR mechanism is thus novel not only in the context of HSR regulation, but also in neural regulation of UPRs broadly. Furthermore, lifespan regulation by CEPsh glial signaling in the cases of the ER (*26*) and mitochondria (*51*) both rely on neuropeptides, which are released via dense core vesicles, whereas the CEPsh glial HSR functions independent of dense core vesicle release. Although neuropeptides are certainly powerful diffusible cues, the HSR data suggest release of neuropeptides is not the automatic glial response to stress across circumstances. Rather, the cells flexibly react to internal states to induce specific programs in distal cells. Thus, the CEPsh glial HSR is not a generalizable alarm system for any potential insult to the cells, but rather specifically induces responses for relevant *hsf-1*-related stressors such as heat and immune challenge.

We find a requirement for the small clear vesicle release protein UNC-13 in the non-cell autonomous communication of the HSR by CEPsh glia; however, the identity of the cue or cues contained in such vesicles remains unclear (Figure 6B). As UNC-13 is thought to be expressed specifically in neurons, the most likely model involves CEPsh glial recruitment of neurons for signaling. We genetically disrupted production or packaging of serotonin, dopamine, octopamine/tyramine, acetylcholine, GABA, and glutamate, and failed to see a robust reduction in HSR signaling. Therefore, these signals could be functioning redundantly to induce the response, another unidentified cargo may be loaded into small clear vesicles, or glia may be modulating neurons in some other way, for example, by reuptake of neurotransmitters. Firstly, a combination of transmitters may act to signal the glial HSR, potentially both acetylcholine and glutamate, for example. Also, distinct non-canonical cues may be at play. A novel small clear vesicle cargo derived from glia or from neurons may be responsible for this signaling. Several distinct stressors have been shown to induce lipids as a glial-neuronal stress signal, for example, which this work cannot rule out (*69–71*). CEPsh glia may also alter neurotransmitter release via damage signals, immune molecules, or even chaperones themselves, though these mechanisms are not well described in the glia of *C. elegans*. Finally, CEPsh glia previously have been shown to alter neuronal activity via neurotransmitter reuptake, particularly in the case of glutamate (*72*). Unexpected baseline increases in thermotolerance and chaperone induction for several neurotransmitter mutants suggest that this is a likely mechanism, as decreases in synaptic levels of such a neurotransmitter could also be responsible for the changes of interest. CEPsh glial *hsf-1* may induce such modulation of neuronal activity via reuptake and could feasibly accomplish non-cell autonomous HSR signaling through these means.

Despite substantial differences in initiation, both the glial and neuronal HSRs converge on the peripheral factors HSF-1 and DAF-16. The whole animal RNA sequencing data presented in this study suggest that *hsf-1* may be transcriptionally upregulated in response to the glial HSR. Less surprisingly, peripheral HSF-1 seems to be required for induction of HSR chaperones, implying activation of the transcription factor's canonical activity in non-glial cells is necessary for the protein homeostasis effects of CEPsh glial *hsf-1*. The beneficial effects of glial *hsf-1* on lifespan are wholly dependent on *hsf-1*, in contrast to the neuronal *hsf-1* model in which HSF-1 is only partially required (*5*). These data suggest that HSF-1 may be an upstream component of the peripheral response, potentially able to activate other beneficial factors downstream. By contrast, the FOXO transcription factor DAF-16, which has been previously implicated in lifespan extension across perturbations including the neuronal HSR, is only partially required for glial *hsf-1* phenotypes (*5*). DAF-16 is canonically repressed by kinases downstream of the insulin receptor DAF-2 as part of the insulin and IGF-1 signaling (IIS) pathway, and activation of DAF-16 is generally correlated with an increase in longevity (*73–75*). In the CEPsh glial *hsf-1* paradigm DAF-16 is at least partially required for lifespan extension, thermotolerance and, to a lesser extent, chaperone induction. However, in all cases a slight increase remains despite peripheral knockdown of *daf-16*, supporting the hypothesis that DAF-16 may be downstream of HSF-1 or other induced protective factors (Figure 6B).

We unbiasedly evaluated whole animal gene expression by RNA sequencing and found a surprising enrichment of immune-related genes upregulated in CEPsh glial *hsf-1* animals. HSF-1 has been previously implicated in immune function, and its role in pathogen resistance is independent of the canonical PMK-1/MAPK innate immune pathway, instead operating in a

chaperone-dependent manner (*68*, *76*). In the worm, infection is a major cause of death, detectable by pharyngeal swelling, and *hsf-1* knockdown increases pharynx bacterial colonization (*67*, *77*). Data here indicate that CEPsh glia are able to induce a pro-immune and pro-longevity program by activating *hsf-1*, possibly increasing cellular protection from pathogens via induction of chaperones and immune response genes. Interestingly, by activating HSF-1-related genes specifically in this paradigm we were able to achieve effective increase of immune function in adult animals without a deleterious effect of prolonged immune activation on longevity. If increased HSF-1 function can protect cells from both proteotoxicity and pathogenic insults, we would anticipate that its activity would be positively selected evolutionarily. However, the negative impact of *hsf-1* upregulation on reproductive function demonstrated here suggests evolutionary titration of function may balance these phenotypes to preserve the health of parents and offspring.

CEPsh glia are well positioned to receive cues from the environment, neurons, and peripheral tissues. This study, along with those detailing the role of these cells in the ER and mitochondrial UPRs, suggests that these cells may act as sensory organs particularly for organismal insults, inducing relevant and specific stress responses across the whole animal (*26*, *51*). The worm has no circulating adaptive immune system; however, the nervous system of *C. elegans* serves as an immune effector, regulating responses to toxic stimuli in coordinated behavioral and cellular programs. The connection between nervous system function and immune signaling in this case points to the larger role of the nervous system itself as the prototype for adaptive immunity.

CEPsh glia are thus able to coordinate multiple protective functions by non-cell autonomous communication of the heat shock response. Considering the aging-related decline of function in the neuronal HSR and its relationship to protein aggregation, manipulation of glial *hsf-1* emerges as a promising tool to tackle aging and neurodegenerative phenotypes broadly.

Methods:

Thermotolerance- Worms were synchronized by bleaching as described here, L1 arrested, and plated on HT115 bacteria. At late D1, 15 worms per plate with 5 plates per condition were exposed to 34ºC heat via incubator for 13-16 hours. Plates were then removed from the incubator and manually assessed for movement and pharyngeal pumping, using light head taps where necessary, to determine survival. Worms that displayed internal hatching or crawled onto the side of the plate and desiccated were censored and omitted from the final analysis. Percent alive was calculated using the number of living worms divided by the total number of worms less censored worms for each strain. Experiments were performed blinded in all cases.

Lifespan- Lifespans were performed as previously described (*26*). In brief, worms were synchronized by bleaching, L1 arrested, and plated on HT115 bacteria. On Day 1 of adulthood, worms were moved to fresh plates with 15 worms per plate and 10 plates per condition. Living worms were counted every day, and occasionally every other day, for the duration of the lifespan. Life was assessed by movement, pharyngeal pumping, or response to a light head touch. Worms were censored if they crawled onto the side of the plate and desiccated, if they displayed internal hatching, or had extruded vulvas/intestines. All lifespans were performed a minimum of three times, excepting the *mir-228* lifespan in Supplementary Figure 2, performed twice. Lifespans were blinded in all cases. Representative experiments are displayed.

Pseudomonas aeruginosa survival: PA14 bacteria was cultured overnight at 37°C protected from light in KB media. 20uL was spread onto slow killing plates, which were incubated 24h at 37°C protected from light. After plates returned to room temperature, synchronized L4 worms were added to the plates, using 6 plates of 20 worms per plate. Survival was assessed as described above. Missing worms and those crawling onto the side of the plate were censored and omitted from analysis, but bagged worms were counted as dead for this assay. Worms were counted at least once per day, but more frequently near peak death. Statistics were performed as described for lifespan experiments.

Imaging: Worms were anesthetized using 100uM sodium azide solution on NGM plates, immediately aligned with a worm pick head to tail and imaged. Fluorescent and brightfield images were collected via the Echo Revolve Microscope. Exposure time and laser intensity were matched within each experiment. For experiments showing extrachromosomal arrays, animals were selected based on the presence of a red co-injection marker while blind to their green fluorescence via the NIGHTSEA benchtop fluorescence adaptor for red fluorescence only. Integrated strain worms were picked for imaging on a non-fluorescent stereoscope to remain blind to green fluorescence.

Worm growth and maintenance: Worms were maintained at 15°C on NGM plates spotted with 200uL of OP50 bacteria. Worms were chunked or picked for experiments onto NGM plates with 1mL OP50 and grown up at 20°C. They were then synchronized for experiments as described here.

Synchronization: Worms were synchronized by bleaching as previously described(*22*). In brief, worms were collected off plates into 15mL conical tubes using M9 solution. Bleach solution was

added until animals dissolved, and the worms were spun down (30s at 1000 RCF) and washed five or more times with M9 before L1 arrest. L1 arrest was performed by suspending worms in M9 in 15mL conical tubes and rotating overnight at 20°C before plating on OP50 or HT115 bacteria.

RNAi feeding: RNAi feeding was performed as previously described (*5*, *78*).

RNA isolation, library preparation, and sequencing: Animals were bleach synchronized and grown to the L4 stage on HT115 plates. At least 2,000 animals per condition per replicate were washed off plates using M9 and collected. After a 30 second spin at 1,000 RCF, M9 was aspirated, replaced with 1mL Trizol, and the tube was immediately frozen in liquid nitrogen to be stored at -80°C for downstream processing. RNA was harvested after 3 freeze thaw cycles in liquid nitrogen/37°C water bath. After the final thaw, 200uL (1:5 chloroform: Trizol) of chloroform solution were added to the sample, vortexed, and the aqueous phase was collected after centrifugation in a gel phase lock tube. RNA was isolated from the obtained aqueous phase using a Qiagen RNeasy MiniKit according to manufacturer's directions. Library preparation was performed by Azenta Genewiz as follows: Extracted RNA samples were quantified using Qubit 2.0 Fluorometer (Life Technologies, Carlsbad, CA, USA) and RNA integrity was checked using Agilent TapeStation 4200 (Agilent Technologies, Palo Alto, CA, USA). RNA sequencing libraries were prepared using the NEBNext Ultra RNA Library Prep Kit for Illumina following manufacturer's instructions (NEB, Ipswich, MA, USA). Briefly, mRNAs were first enriched with Oligo(dT) beads. Enriched mRNAs were fragmented for 15 minutes at 94°C. First strand and second strand cDNAs were subsequently synthesized. cDNA fragments were end repaired and adenylated at 3'ends, and universal adapters were ligated to cDNA fragments, followed by index addition and library enrichment by limited-cycle PCR. The sequencing libraries were validated on the Agilent TapeStation (Agilent Technologies, Palo Alto, CA, USA), and quantified by using Qubit 2.0 Fluorometer (Invitrogen, Carlsbad, CA) as well as by quantitative PCR (KAPA Biosystems, Wilmington, MA, USA). The sequencing libraries were clustered on one lane of a flow cell. After clustering, the flow cell was loaded on the Illumina HiSeq instrument (4000 or equivalent) according to manufacturer's instructions. The samples were sequenced using a 2x150bp Paired End (PE) configuration. Image analysis and base calling were conducted by the HiSeq Control Software (HCS). Raw sequence data (.bcl files) generated from Illumina HiSeq was converted into fastq files and de-multiplexed using Illumina's bcl2fastq 2.17 software. One mismatch was allowed for index sequence identification.

RNA sequencing analysis: For RNA-seq analysis, the sequencing data were uploaded to the Galaxy project web platform and the public server at *usegalaxy.org* was used to analyze the data (*79*). Paired end reads were aligned using the Kallisto quant tool (Version 0.46.0) with WBcel235 as the reference genome. Fold changes and statistics were generated using the DESeq2 tool with Kallisto quant count files as the input. Volcano plots were generated using GraphPad Prism software (Version 9.2.0 (283)) on the fold change and adjusted-p values generated by the previous analysis. GO terms for differentially expressed genes were analyzed by using the GOrilla tool (http://cbl-gorilla.cs.technion.ac.il/#ref) on lists of genes that were up or down regulated (Log2FC > 1, <1, respectively) with an adjusted P-value <= 0.05 (*66*, *80*). The raw RNA-seq data were uploaded to the NCBI short read archive (PRJNA801195). Access for reviewers is available at

https://dataview.ncbi.nlm.nih.gov/object/PRJNA801195?reviewer=9jun897nhgr342vonpa0v3a49p .

Generation and integration of arrays: The *hlh-17* promoter was cloned into a vector containing full length *hsf-1*, with sequences as previously described (*5*, *26*). Wild type N2 strain worms were injected with the *hlh17p::hsf*-1; *unc-54* 3'UTR plasmid and *myo-2p::tdtomato* co-injection marker. Integration of extrachromosomal array lines was performed by gamma irradiation (*Is2(hlh-17p::hsf-1)*) or by UV irradiation (*Is1(hlh-17p::hsf-1)*). Integrated lines were then backcrossed at least eight times to the wild type N2 strain. Due to rapid transgene suppression of the integrated strains, the extrachromosomal array was used in all cases involving crosses, excepting data in Supplementary Figure 1E and F and Supplementary Figure 5. Integrated strains were also used for all lifespans and for thermotolerance data in Supplementary Figure 1D, as well as for RNA sequencing.

Brood size: Synchronized L4 animals were picked individually onto fresh HT115 bacteria plates and allowed to lay eggs for 24h at 20°C. They were then moved to fresh plates for each consecutive 24h period for the duration of the reproductive lifespan for at least five days. Progeny plates were allowed to grow up at 20°C for two days, and surviving larvae were imaged using the MBF Bioscience WormLab imaging system and counted.

Heat shock for imaging: Synchronized worms were placed in a 34°C incubator for 2h, followed by a recovery for 2h at 20°C, at which time worms were imaged or biosorted as described.

Prediction of HSF-1 binding sites in *C. elegans* promoters: HSF-1 binding sites were predicted in the upstream regions of coding sequences using the FIMO tool (version 5.0.5) on MEME Suite (*81*, *82*). Briefly, 500bp upstream flanks of all annotated coding genes were downloaded from the WormBase ParaSite to represent putative promoter regions (*83*). The HSF-1 position weight matrix (PWM) was downloaded from JASPAR (matrix ID MA0486.2) (*84*). FiMO was run with the HSF-1 PWM as input motif and the putative promoter regions as input sequences with a match P-value < 1E-5 to find 646 genes with HSF-1 binding sites. GO term analysis using the GOrilla tool confirmed the top GO terms of these genes to include chaperone mediated folding (GO:0061077), protein folding (GO:0006457) and response to heat (GO:009408).

COPAS biosorting and analysis: Worm sorting using the COPAS biosorter (Union Biometrica) was performed as previously described (*22*). In brief, worms were heat shocked as described for *hsp-16.2p::GFP* conditions. Then, they were washed off plates into the sample cup using M9 and sorted. Laser PMT values were consistent within experiments. All raw data was saved. For analysis, reads with time of flight (TOF) greater than 100 and extension (EXT) greater than 50 were included and reads with lower values were excluded. Reads for which EXT or green peak height reached the maximum saturated value of 65532 were excluded. Normalized fluorescence was calculated by dividing green peak height by TOF. For red-headed animals, worms with a red peak height of 1000 or greater were included, and lower values were presumed extrachromosomal array negative and were excluded.

Genetic crosses: Males were generated either by heat exposure or by crossing to wild type males. Hermaphrodites and males of interest were placed on NGM plates with a small amount of OP50

bacteria and allowed to mate. Progeny were singled onto individual plates for the F1 and the subsequent F2 generation and were screened for relevant phenotypes.

Statistical analyses: Statistical analysis was performed using GraphPad Prism 9.2.0(283), excepting RNA sequencing analysis which was performed as described above. Individual analyses are as described in figure legends. Lifespans were analyzed by Gehan-Breslow-Wilcoxon test. Two condition comparisons were otherwise analyzed by two-tailed t test, with Welch's correction where applicable, and more than two condition comparisons were analyzed by one-way ANOVA with Sidak's multiple comparisons. The brood size assay experiment was analyzed via a Kolmogorov-Smirnov test due to our inability to assume a Gaussian distribution.

Chapter 3: Endogenous roles of CEPsh glia in *C. elegans* heat shock response function

Introduction:

In mammals, glial central nervous system cell types include astrocytes, microglia, and oligodendrocytes. Astrocytes are best known for their metabolic support of neurons, shuttling nutrients and necessary ions from the periphery into the central nervous system. They also contribute coordinated electrical signaling in the form of calcium waves, which correlates with higher order neural functions (*85*). Astrocytes are highly interactive with neurons, responding to electrical activity by supplying neurotransmitter intermediates and by dynamically regulating metabolic coupling. Mammalian astrocytes are also highly stress sensitive, and can physically remove damage from neurons in some cases (*48*, *49*).

In the nematode *C. elegans* there are 56 glia, relative to 302 neurons and nearly 1000 somatic cells(*21*). Of the 56, 6 are mesodermally derived; the others are ectodermally derived (*21*). Among the ectodermal cells, many function in the physical anchoring of neurons and tissues along the worm, but also serve many traditional glial-specific functions. Four cells, the cephalic sheath or CEPsh glia, are best known for their astrocyte-like roles (*21*). Much like mammalian astrocytes, they participate heavily in separation of the nerve ring, the *C. elegans* brain-like CNS center, from surrounding tissues (*86*). CEPsh cells also help direct neuronal development and synapse formation, and they remain present at synapses in the manner of the canonical "tripartite synapse" formed by astrocytes and neurons in mammals (*21*, *87*). These cells also express many characteristic astrocytic genes, including GLAST ortholog GLT-1(*72*). Interestingly, in addition to astrocytic functions, CEPsh cells may also be early evolutionary examples of oligodendrocyte-like cells, as they both ensheath neuronal sensory processes that project into the periphery and are characterized by expression of the canonical oligodendrocyte gene *Olig2*, *hlh-17* (*21*). In sum, CEPsh cells are morphologically, functionally, and genetically similar to mammalian CNS, ectodermally-derived glia, particularly astrocytes.

The endogenous roles for CEPsh glia primarily have been determined using developmental mutants in their specification. The transcription factor *hlh-17* is uniquely expressed in CEPsh glia (*26*, *88*). The two ventral and two dorsal CEPsh glia are specified by a similar but distinct cascade of transcription factors that lead to upregulation of *hlh-17* itself (*89*). In ventral CEPsh glia, the transcription factor *vab-3* activates the transcription factor *mls-2*, both of which are required for downstream induction of *hlh-17* (*89*). Dorsally, however, CEPsh glia require only *vab-3*, not *mls-2*, for CEPsh glial specification (*89*). Morphological defects in CEPsh glia and in their projections surrounding sensory processes have been observed in *vab-3* and *mls-2* mutant animals, specifically in the two ventral CEPsh glia in *mls-2* mutants, while *vab-3* mutation impacts the formation of all four cells (*89*).

In addition, previous work has used an *hlh-17* promoter-driven reconstituted caspase in order to ablate CEPsh cells (*26*, *90*). This system allows the post-developmental ablation of all four CEPsh cells, in order to probe additional functions. Under this system, we now know that CEPsh glia are required for proper sleep-related molting phenotypes in the worm via electrical control of ALA and AVE neurons (*90*). They also modulate the dopaminergic CEP cells with which they interact (*91*).

As we established above, CEPsh cells have unique signaling mechanisms that enable them to signal organelle stress to peripheral tissues (*24, and Chapter 2*). Less understood is the role of CEPsh glia in regulating stress under basal conditions. Frakes et al. demonstrate that ablation of CEPsh glia by caspase does not itself decrease or increase lifespan (*26*). However, the work also shows that without CEPsh glia, animals are particularly sensitive to ER stress (*26*). These data suggest that either ER stress is not a central determinant of lifespan in these animals, which we doubt due to its importance in proteostasis, or that there are other beneficial effects on lifespan generated through separate means.

Additionally, nothing is yet known about the role of CEPsh glia in HSR management under basal conditions. We have established that CEPsh cells are able to non-autonomously regulate the HSR, but we do not know if HSR functions are impaired or altered in their absence. Further, although we potentially implicate neurotransmitter signaling as a non-autonomous signaling mechanism of the CEPsh glial HSR, we have yet to describe effects of CEPsh-neuronal interactions on HSR functions. Here, we endeavor to answer these questions.

Results:

We first characterized variability in CEPsh glial specification and morphology in the *vab-3* and *mls-2* mutant strains by imaging of an *hlh-17p::GFP* reporter animal (Figure 7). These mutants have been previously thoroughly characterized for penetrance (*89*). After backcrossing the strains to our own wild-type N2 strain, we confirmed previous findings suggesting that *vab-3* mutants caused a more complete deficit in both ventral and dorsal CEPsh glial morphology than *mls-2* mutants, for which only ventral morphology was perturbed, in the *hlh-17p::GFP* reporter animals (Figure 7). In our hands, however, we found that the *vab-3(ju468)* mutation caused more complete failure to ensheath the nerve ring and failure to extend distal processes than the *vab-3(e648)* mutation, though both *vab-3* strains exhibited deficits in all four CEPsh cells (Figure 7).

Figure 7

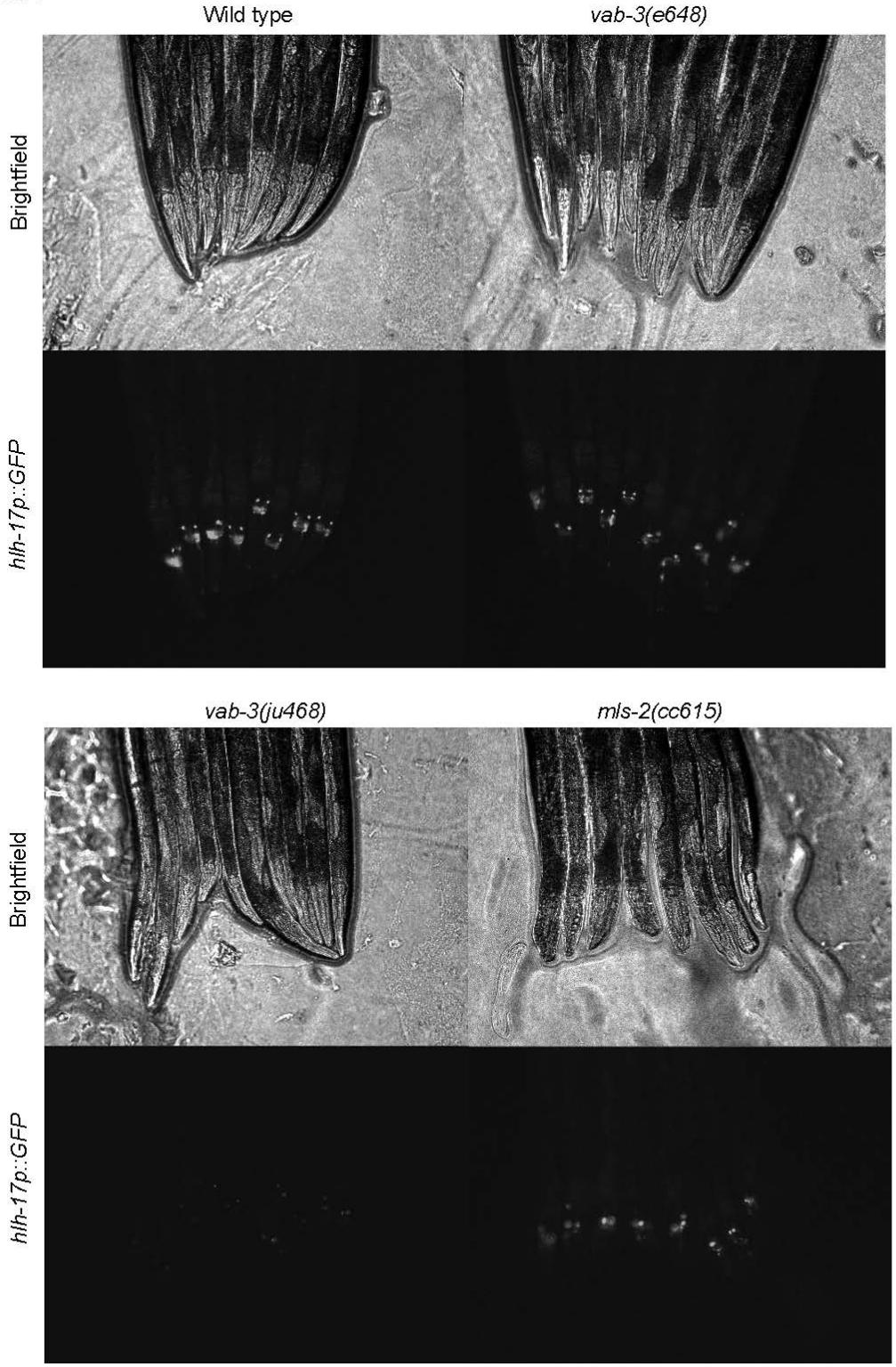

Figure 7: *hlh-17p::GFP* images of heads of worms reveal CEPsh glial morphology. Top left: wild type animals with CEPsh glia labeled by *hlh-17p::GFP*. Top right: *vab-3(e648)* mutants show partial disruption with incomplete penetrance of all four CEPsh glia. Bottom left: *vab-*

39ju468) mutants exhibit near complete ablation of labeling by *hlh-17p::GFP* and have no obvious nerve ring wrapping or outgoing sensory process ensheathment. Bottom right: *mls-2(cc615)* mutants show disruption in two out of four CEPsh cells.

In addition to these mutants, we used the *hlh-17p::recCaspase* strain previously characterized by Frakes et al (*26*). This mutant has a similar level of morphological deficit to the *vab-3(ju468)* strain, but as *vab-3* is upstream of *hlh-17* activation, the caspase strain results in ablation of the CEPsh cells after their specification, later in the developmental timeline of the animal. In this work we use all of the described ablation and developmental mutant strains. Notably for later analysis, however, *mls-2* mutants perturb only ventral cells while *vab-3* mutants perturb all four. Further, the caspase strain perturbs CEPsh glia post-developmentally, while *vab-3* and *mls-2* mutants affect the cells during specification.

As animals lacking CEPsh glia are sensitive to ER stress but show no decline in lifespan, we next wondered whether these animals were uniformly sensitive to stressors, or whether dynamic regulation of individual responses might account for the lack of lifespan phenotype. To evaluate this, we turned our attention to the heat shock response (HSR). In Chapter 2, we established that over-expression of the main HSR regulator, heat shock factor 1 (*hsf-1*), in CEPsh glia was able to increase stress tolerance and lifespan through non-cell autonomous communication. We next wondered whether CEPsh glia served an endogenous role in regulation of HSR function or heat stress tolerance.

We performed the thermotolerance assay on *vab-3(ju468)* and *vab-3(e648)* animals lacking all CEPsh glia, *mls-2(cc615)* animals lacking only two of the CEPsh glia, and wild type animals. We found that both *vab-3* mutant strains, but not the *mls-2* strain, exhibited a slight but consistent increase in thermotolerance relative to wild type animals (Figure 8A). Across trials, despite the variability of the thermotolerance assay, *vab-3(ju468)* thermotolerance was significantly increased relative to wild type, while *mls-2(cc615)* thermotolerance was not significantly different than wild type (Figure 8B). These data suggest that ablation of all four CEPsh glia is required to induce a thermotolerance increase, and the ablation of two cells is insufficient. Unfortunately, there is no converse mutation to *mls-2* that would delete specifically dorsal CEPsh, so we cannot discriminate between a requirement for all four cells and a requirement for the dorsal CEPsh glia particularly. In sum, survival under chronic heat stress does not require the presence of CEPsh glia, but rather these cells may serve a role in dynamic regulation of the HSR.

We next asked whether this alteration in thermotolerance was the result of an increase in basal chaperone levels. To assess this, we measured the fluorescence of the *hsp-16.2p::GFP* transcriptional reporter for *hsp-16.2* in *vab-3(ju468)* animals versus wild type. We found that the *vab-3* animals showed no increase in *hsp-16.2*, and rather exhibited a potential decrease (Figure 8C). This suggests that increased chaperone expression upon heat shock cannot explain the increase in thermotolerance caused by *vab-3*-mediated glial ablation.

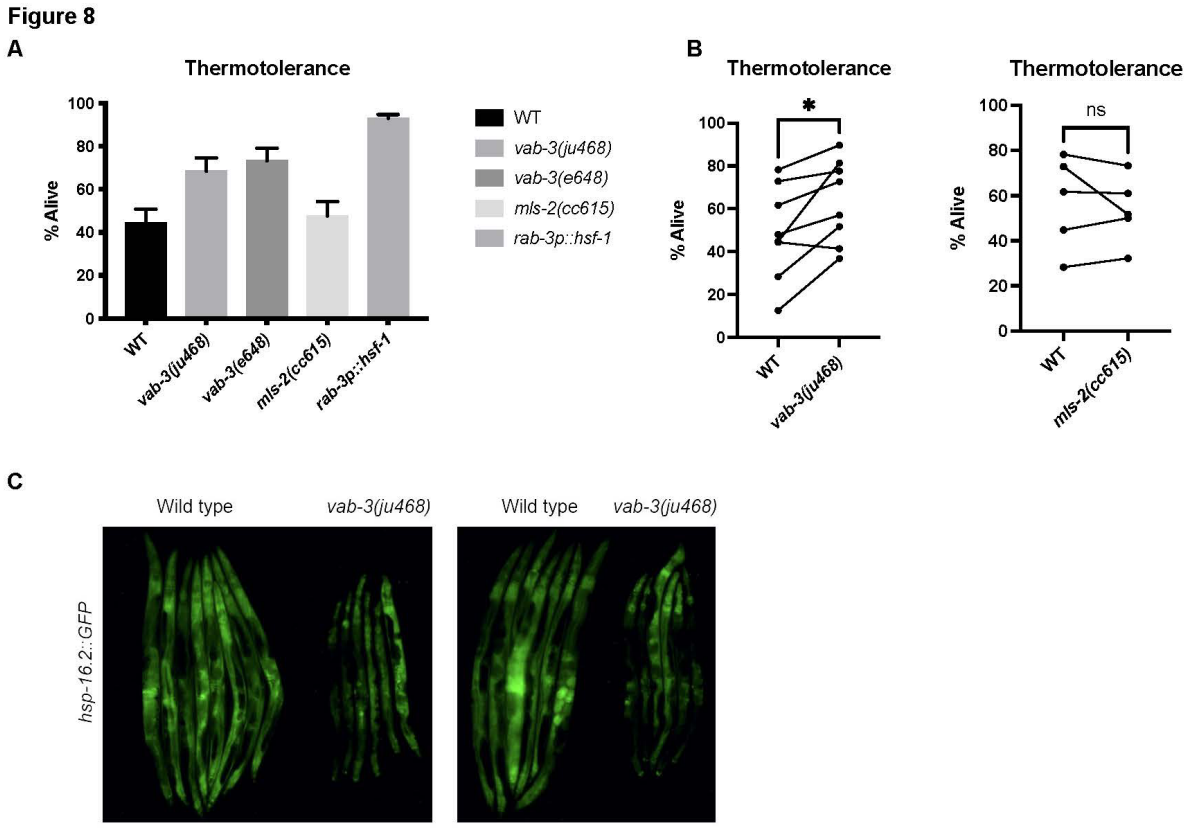

Figure 8: CEPsh glial ablation alters thermotolerance and chaperone induction under heat. A) Representative thermotolerance data for both *vab*-3 mutant strains alongside the *mls-2* mutant strain and the neuronal *hsf-1* overexpressor (2-3 experiments per condition, error bars =SD, n=150 or 225, 75 per experiment number) B) Thermotolerance data across trials for *vab-3(ju468)* (left) and *mls-2(cc615)* (right). Experiments are connected points; n within experiments = 75 per condition. Thermotolerance of *vab-3(ju468)* is greater than wild type, $p<0.05$, and *mls-2(cc615)* is not significantly changed, by two-tailed t test. C) Imaging for the reporter strain *hsp-16.2p::GFP* after 2h heat shock and 2h recovery with potential decrease in *vab-3(ju468)* strains relative to wild type (n= 3 experiments).

Having identified a role for CEPsh glia in dynamic regulation of the HSR, we next tested whether CEPsh glia might be required for the survival and stress tolerance benefits conferred by neuronal over-expression of *hsf-1*. We crossed the original, unbackcrossed, glial caspase strain into the *rab-3p::hsf-1* neuronal over-expression strain and evaluated the lifespan of the animals. Despite the relative increase in lifespan caused by not backcrossing the glial caspase strain, we found that *rab-3p::hsf-1* animals lacking CEPsh glia did not display a lifespan extension similar to *rab-3p::hsf-1* animals alone (Figure 9A). We next tested thermotolerance of these animals. Notably, glial caspase animals did not display an obvious increase in thermotolerance relative to wild type animals, in a divergence from the *vab-3* method of glial ablation, suggesting that the observed *vab-3* effects on lifespan may be developmental in nature (Figure 9B). We also

confirmed that *rab-3p::hsf-1* animals were thermotolerant relative to wild type animals, as previously reported (Figure 9B). However, despite an increase in thermotolerance in neuronal *hsf-1* animals and no decrease in thermotolerance in glial caspase animals, when combined the neuronal *hsf-1* glial caspase animals exhibited a decrease in thermotolerance and were visibly synthetically sick (Figure 9B). We next tested whether ablation of CEPsh glia by *vab-3(ju468)* was sufficient to recapitulate this effect. When *rab-3p::hsf-1* animals were crossed into *vab-3(ju468)* animals, rather than exhibiting an increase in thermotolerance, they in fact showed a decrease (Figure 9C). Taken together, these data suggest that CEPsh glia are required for the survival and stress-tolerance benefits of neuronal over-expression of *hsf-1*, and that ablation of CEPsh glia in these strains leads to synthetically sick phenotypes.

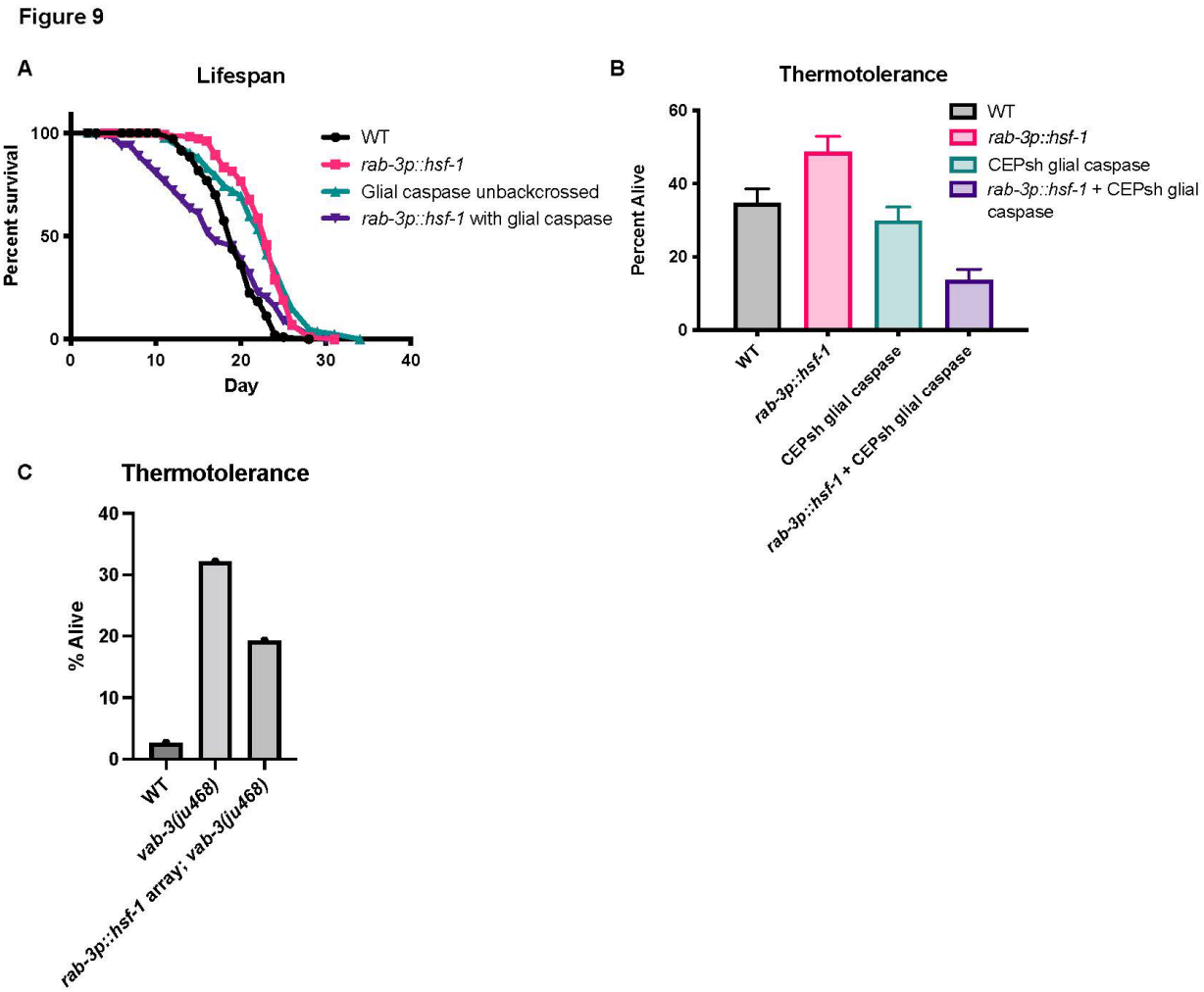

Figure 9: CEPsh glia are required for neuronal *hsf-1* beneficial phenotypes A) Lifespan of *rab-3p::hsf-1* (pink) is significantly increased ($p<0.0001$) versus wild type (black). *rab-3p::hsf-1* with CEPsh glial caspase (purple) is significantly decreased relative to wild type (black) ($p=0.02$). Lifespan medians: WT = 19 days, *rab-3p::hsf-1* = 23 days, CEPsh glial caspase unbackcrossed= 23 days, *rab-3p::hsf-1* with CEPsh glial caspase= 17 days. B) Thermotolerance

of *rab-3p::hsf-1* (pink) is significantly increased vs WT (gray) ($p<0.0001$), while thermotolerance of *rab-3p::hsf-1* with CEPsh glial caspase is significantly decreased vs. WT (purple) ($p<0.0001$) (n=75, error bars =SD) C) Thermotolerance of *rab-3p::hsf-1* with *vab-3(ju468)* is significantly decreased relative to *rab-3p::hsf-1* alone ($p<0.0001$) (n=75)

Discussion:

We here show that disruption of CEPsh glia leads to perturbances of HSR function in a mutant-specific manner. Here, we characterize by imaging several developmental mutants for morphological phenotypes of CEPsh glia and further use. We demonstrate that mutation of all four CEPsh glia, but not two of the four cells, can lead to increased thermotolerance without increasing chaperone induction. Further, we show that CEPsh glia are required for neuronal HSR signaling-based stress tolerance and lifespan phenotypes.

We previously showed that CEPsh glial *hsf-1* is sufficient to induce HSR signaling (Chapter 2); however, the works presented in this chapter are the first to our knowledge to demonstrate a requirement for CEPsh cells in normal levels of HSR function. The data presented here imply that CEPsh glia do, indeed, play an endogenous role in regulation of this signaling and responsiveness. Interestingly, ablation and hyper-activation of CEPsh cells or their HSR functions, respectively, do not lead to opposing phenotypes. Such findings suggest multiple possibilities. In one case, we can imagine that CEPsh glia may dynamically regulate HSR induction levels, by either activating the response in the case of immune insult, protein misfolding, or relevant heat stress, or by providing negative feedback on the response when HSR signaling is over-activated. In this case, we would expect that CEPsh glia may induce *hsf-1*-related signaling, the mechanisms of which we describe in Chapter 2, upon acute stress to aid the activation of a protective peripheral response. However, if signaling is prolonged or severe, CEPsh glia may function in a negative feedback manner to down-regulate neuronal signaling of the HSR. In this case, we would expect that CEPsh glia sense neuronal activation of the response through some externalized cue, damage marker, or glial internal state sensing when over-activated. It remains unclear whether these two responses, upregulation and downregulation of the HSR, are connected at all or require the same mechanisms, though these works suggest compelling areas for further study.

In another case, these phenotypes may be completely differentiable. We know that CEPsh glial *hsf-1* is sufficient to induce the HSR throughout the animal but have not shown effects of direct manipulation of *hsf-1* in these cells. The ablation of CEPsh glia is known to cause several neural development defects, though many of these functions have been specifically attributed to ventral CEPsh glia (*89*). Neuronal dysfunction is likely to result downstream of these perturbances, nonetheless. The canonical mechanism of non-cell autonomous HSR communication by neurons relies on activation of the AFD sensory neuron, the AIY interneuron, and downstream HSN and NSM serotonergic neurons (*17*, *18*). If the cells failed to develop completely, we would expect defects in thermotolerance to occur. Instead, negative regulators of the pathway may be impacted, or the neurons may become hyperactive without regulation by CEPsh glia. As we fail to see an increase in thermotolerance in the CEPsh glial caspase strains, which eliminate the cells after the activation of *hlh-17* itself, the effect observed in the *vab-3* strains likely results from an early developmental impact on the system, supporting this later hypothesis.

Developmental mutation of all four CEPsh cells via two *vab-3* mutations mildly but consistently increases thermotolerance relative to wild-type animals. However, disruption of only the ventral cells via *mls-2* mutant does not lead to this phenotype. Due to the lack of a mutant

perturbing only dorsal development, we cannot identify whether this observation stems from a sufficiency of *mls-2*-negative dorsal CEPsh cells to supplement for the loss of their dorsal counterparts when two cells are present or from a specific requirement for dorsal cells cells in HSR regulation. Dorsal-specific CEPsh mutants or interrogation tools would be necessary to disambiguate these possibilities. However, we can eliminate previously described ventral CEPsh glial mutant axon guidance phenotypes from possible causes of thermotolerance change (*89*).

Interestingly, ablation of CEPsh cells causes sensitivity to ER stress, while here we see an increase in tolerance to heat stress (*26*). These diverging effects may explain why we also observe no overt increase or decrease in lifespan in these animals (*26*). Potentially these data reflect differential regulation of specific organelle stress responses. In the case of heat stress this may be more dynamic than with ER stress.

We also identified a requirement for CEPsh glia in the neuronal *hsf-1*-based non-cell autonomous HSR phenotypes. This total requirement for both lifespan and thermotolerance was unexpected, as previous work with the neuronal *hsf-1* strain demonstrated only a partial requirement for the thermo-signaling AIY interneuron itself, for thermotolerance but not for lifespan extension (*5*). These data suggest that CEPsh glia are upstream of a divergent pathway including AIY for thermotolerance increase and another mechanism for lifespan extension. This interaction could be specific to thermosensory pathways or instead alter their activity by generally perturbing neural development. However, as CEPsh glial ablation strains themselves, either *vab-3*, *mls-2*, or glial caspase, do not exhibit shortened or extended lifespan, we expect that there is likely some specificity in the affected cells (*26*).

Interestingly, CEPsh glial ablation in the neuronal *hsf-1* strains seems not only to abrogate increase in lifespan and stress tolerance, but also cause synthetic sickness and vulnerability. These data suggest that neuronal *hsf-1* animals may rely on CEPsh glia for a specific supportive function when under the imposed stress. One hypothesis would suggest that HSR-signaling neurons may increase electrical activity, consequently increasing their need for supportive metabolic functions of the astrocyte-like CEPsh cells in breaking down glutamate to avoid excitotoxicity. In this case, normally functioning neurons would not require the presence of CEPsh glia for survival, as in the normally survived glial ablation strains, and neurons under stress of *hsf-1* in the presence of CEPsh glia would be well supported. However, under *hsf-1* stress without CEPsh cells present, neurons would then experience toxicity. We have begun to evaluate this possibility by use of null alleles for CEPsh glial glutamate transporters. However, based on preliminary data it seems such mutation cannot recapitulate the sickness observed in CEPsh glial ablation neuronal *hsf-1* animals. More work is needed to understand how CEPsh glia may be supporting neurons under stressed conditions.

Taken together, these data provide the first evidence of a requirement for CEPsh glia in heat stress signaling regulation. Further, the requirement for CEPsh glia in neuronal *hsf-1* signaling leads to interesting avenues of further study.

Methods:

Thermotolerance- Worms were synchronized by bleaching as described here, L1 arrested, and plated on HT115 bacteria. At late D1, 15 worms per plate with 5 plates, thus n=75, per condition were exposed to 34ºC heat via incubator for 13-16 hours. Plates were then removed from the incubator and manually assessed for movement and pharyngeal pumping, using light head taps where necessary, to determine survival. Worms that displayed internal hatching or crawled onto the side of the plate and desiccated were censored and omitted from the final analysis. Percent alive was calculated using the number of living worms divided by the total number of worms less censored worms for each strain. Experiments were performed blinded in all cases.

Lifespan- Lifespans were performed as previously described (*78*). In brief, worms were synchronized by bleaching, L1 arrested, and plated on HT115 bacteria. On Day 1 of adulthood, worms were moved to fresh plates with 15 worms per plate and 10 plates per condition, thus n=150 animals per condition. Living worms were counted every day, and occasionally every other day, for the duration of the lifespan. Life was assessed by movement, pharyngeal pumping, or response to a light head touch. Worms were censored if they crawled onto the side of the plate and desiccated, if they displayed internal hatching, or had extruded vulvas/intestines. Lifespans were blinded in all cases.

Imaging: Worms were anesthetized using 100uM sodium azide solution on NGM plates, immediately aligned with a worm pick head to tail and imaged. Fluorescent and brightfield images were collected via the Echo Revolve Microscope or a Leica M205FA. Exposure time and laser intensity were matched within each experiment.

Worm growth and maintenance: Worms were maintained at 15°C on NGM plates spotted with 200uL of OP50 bacteria. Worms were chunked or picked for experiments onto NGM plates with 1mL OP50 and grown up at 20°C. They were then synchronized for experiments as described here.

Synchronization: Worms were synchronized by bleaching as previously described(*22*). In brief, worms were collected off plates into 15mL conical tubes using M9 solution. Bleach solution was added until animals dissolved, and the worms were spun down (30s at 1000 RCF) and washed five or more times with M9 before L1 arrest. L1 arrest was performed by suspending worms in M9 in 15mL conical tubes and rotating overnight at 20°C before plating on OP50 or HT115 bacteria.

RNAi feeding: RNAi feeding was performed as previously described (*5*, *78*).

Heat shock for imaging: Synchronized worms were placed in a 34°C incubator for 2h, followed by a recovery for 2h at 20°C, at which time worms were imaged or biosorted as described.

Genetic crosses: Males were generated either by heat exposure or by crossing to wild type males. Hermaphrodites and males of interest were placed on NGM plates with a small amount of OP50 bacteria and allowed to mate. Progeny were singled onto individual plates for the F1 and the subsequent F2 generation and were screened for relevant phenotypes.

Statistical analysis: Statistical analysis was performed using Graphpad Prism 9.2.0(283). Individual analyses are as described in figure legends. Lifespans were analyzed by Gehan-Breslow-Wilcoxon test. Two condition comparisons were otherwise analyzed by two-tailed t test.

Chapter 4: Conclusion

Taken together, the data presented here demonstrate a novel role for the CEPsh glia of *C. elegans* in inducing and maintaining the HSR. We show both endogenously and with *hsf-1* overexpression that CEPsh cells can modulate organismal protein homeostasis, to the same extent with just four glial cells as with all 302 neurons.

Firstly, we demonstrate that over-expression of *hsf-1* in the four CEPsh glia of the worm causes an increase in lifespan and heat stress tolerance and causes non-cell autonomous induction of the HSR both by *hsp-16.2* reporter under stress and basally by sequencing. This is not purely the same response as that induced by neuronal *hsf-1*. In fact, both the AIY interneuron and serotonin synthesis are dispensable for this response. The independence of serotonin, which coordinates all known neuronal non-autonomous UPR signaling, is particularly notable (*18*, *34*, *35*). Downstream changes in metabolic and overall cellular functions are both similar and distinct from the neuronal model. In both cases, *hsf-1* is peripherally required (*5*). In the glial case, *daf-16* is partially required, while it is fully necessary for lifespan effects in the neuronal model (*5*). We also noted the robust upregulation of immune factors in CEPsh glial *hsf-1* animals and found that this correlated with increased immune function. As these animals did not broadly upregulate all stress responses, we propose that this immune function increase is a coordinated response to pathogen infection as an HSR stressor. The non-canonical immune response initiated by glial *hsf-1* suggests interesting future areas of study in the HSF-1-mediated, pro-longevity immune response.

We also establish an endogenous responsibility for heat stress management in CEPsh cells. We use three different mutation strategies for CEPsh glia: *vab-3* mutation (all 4 cells affected), *mls-2* mutation (2 ventral cells affected), and a caspase expressed under the *hlh-17* promoter (all 4 cells affected). Surprisingly, we find that developmental mutation of all four CEPsh glia via *vab-3* mutation increases thermotolerance relative to wild type, whereas mutation of only 2 cells via *mls-2* is insufficient. These data suggest that the presence of CEPsh glia plays some role in regulation of HSR function under chronic or severe conditions. Interestingly, we failed to observe an increase in the chaperone *hsp-16.2* in *vab-3* mutant animals, perhaps even observing a decrease in the chaperone. Together, these data suggest that CEPsh glia may dynamically regulate the HSR, providing both activating and inhibiting functions in a situation-dependent manner. However, our works here have not elucidated the circumstances under which such signaling may occur in each direction. Interestingly, we also find that CEPsh glia are fully required for the neuronal *hsf-1* over-expression's beneficial phenotypes of stress resistance via thermotolerance and lifespan extension. Given that the neuronal signaling of thermotolerance and lifespan is thought to rely on two distinct pathways, these data suggest that CEPsh glia lay at a more upstream point, potentially regulating neuronal health and activity. Therefore, we hypothesize that the neuronal dependence on CEPsh glia may operate through a different pathway than CEPsh glial *hsf-1* overexpression, perhaps via a lack of structural or metabolic support to neurons.

Future research concerning the relationship between glial and neuronal heat stress is necessary. Firstly, in both the case of the neuronal HSR and glial HSR the diffusible cue or exact pattern of neuronal activity is not yet identified. Finding such a cue or cues will both aid in our understanding of the system and provide important points of manipulation to identify whether this pathway is conserved in mammals and whether it has therapeutic potential for treatment of

protein misfolding diseases. Additionally, we must better understand the interactions, both physical and signaling-based, between CEPsh glia and neurons as animals age. These works will aid in our broader understanding of conserved glial-neuronal interactions.

Overall, these findings shed light on a previously unstudied set of characteristics for CEPsh glia, that of their roles in the HSR. As we learn more about glial-neuronal interactions in both *C. elegans* and mammals, we hope to identify more ways in which we can modulate this signaling to improve organismal health. Identification of such pathways will hopefully provide future avenues for anti-aging and anti-neurodegenerative therapeutics.

Table 1: Strain List

STRAIN	SOURCE	IDENTIFIER
C. elegans: strain N2 (Bristol)	CGC	N2
C. elegans: strain AGD2899, *uthls490[hlh-17p::hsf-1 FL::unc-54 3'UTR, myo-2p::tdTomato]*	This paper	AGD2899; in this paper *Is1(hlh-17p::hsf-1)*
C. elegans: strain AGD2007, *uthEx861[hlh-17p::hsf-1 FL::unc-54 3'UTR, myo-2p::tdTomato]*	This paper	AGD2007; in this paper *Ex(hlh-17p::hsf-1)*
C. elegans: strain AGD2008, *uthEx861[hlh-17p::hsf-1 FL::unc-54 3'UTR, myo-2p::tdTomato];dvln70[pCL25 (hsp-16.2p::GFP), pRF4(rol-6)]*	This paper	AGD2008
C. elegans: strain CL2070, *dvln70[pCL25 (hsp-16.2p::GFP), pRF4(rol-6)]*	CGC	CL2070
C. elegans: strain FK134, *ttx-3(ks5) X*	CGC	FK134
C. elegans: strain AGD3250, *ttx-3(ks5) X; dvln70[pCL25 (hsp-16.2p::GFP), pRF4(rol-6)]*	This paper	AGD3250
C. elegans: strain AGD3055, *uthEx861[hlh-17p::hsf-1 FL::unc-54 3'UTR, myo-2p::tdTomato];dvln70[pCL25 (hsp-16.2p::GFP), pRF4(rol-6)]; ttx-3(ks-5)*	This paper	AGD3055
C. elegans: strain MT15434, *tph-1(mg280)II*	CGC	MT15434
C. elegans: strain AGD3254, *tph-1(mg280)II; dvln70[pCL25 (hsp-16.2p::GFP), pRF4(rol-6)]*	This paper	AGD3254
C. elegans: strain AGD3056, *uthEx861[hlh-17p::hsf-1 FL::unc-54 3'UTR, myo-2p::tdTomato]; dvln70[pCL25 (hsp-16.2p::GFP), pRF4(rol-6)]; tph-1(mg280)*	This paper	AGD3056

C. elegans: strain AGD1989, *unc-13(s69) I*, EG9631 backcrossed	CGC and Frakes et al. 2020	AGD1989
C. elegans: strain AGD3113, *dvln70[pCL25 (hsp-16.2p::GFP), pRF4(rol-6)]; unc-13(s69) I.*	This paper	AGD3113
C. elegans: strain AGD3115, *uthEx861[hlh-17p::hsf-1 FL::unc-54 3'UTR, myo-2p::tdTomato]; dvln70[pCL25 (hsp-16.2p::GFP), pRF4(rol-6)]; unc-13(s69) I*	This paper	AGD3115
C. elegans: strain CB928, *unc-31(e928)IV.*	CGC	CB928
C. elegans: strain AGD3054, *dvln70[pCL25 (hsp-16.2p::GFP), pRF4(rol-6)]; unc-31(e928)IV.*	This paper	AGD3054
C. elegans: strain AGD3114, *uthEx861[hlh-17p::hsf-1 FL::unc-54 3'UTR, myo-2p::tdTomato]; dvln70[pCL25 (hsp-16.2p::GFP), pRF4(rol-6)]; unc-31(e928)IV*	This paper	AGD3114
C. elegans: strain AGD3029, *eat-4(ky5) III* backcrossed	CGC and Dillin Lab	AGD3029
C. elegans: strain AGD3268, *uthEx861[hlh-17p::hsf-1 FL::unc-54 3'UTR, myo-2p::tdTomato]; eat-4(ky5) III.*	This paper	AGD3268
C. elegans: strain AGD3038, *tdc-1(n3419) II* backcrossed	CGC and Dillin Lab	AGD3038
C. elegans: strain AGD3267, *uthEx861[hlh-17p::hsf-1 FL::unc-54 3'UTR, myo-2p::tdTomato]; tdc-1(n3419) II*	This paper	AGD3267
C. elegans: AGD3159, *unc-17(e245) IV* backcrossed	CGC and Dillin Lab	AGD3159
C. elegans: AGD3255, *unc-17(e245) IV; uthEx861[hlh-17p::hsf-1*	This paper	AGD3255

FL::unc-54 3'UTR, myo-2p::tdTomato]		
C. elegans: strain MT15620, *cat-2(n4547) II*	CGC	MT15620
C. elegans strain AGD3253, *cat-2(n4547) II; uthEx861[hlh-17p::hsf-1 FL::unc-54 3'UTR, myo-2p::tdTomato]*	This paper	AGD3253
C. elegans: strain AGD3161, *unc-25(e156) III* backcrossed	CGC and Dillin Lab	AGD3161
C. elegans: AGD3201, *uthEx861[hlh-17p::hsf-1 FL::unc-54 3'UTR, myo-2p::tdTomato]; unc-25(e156) III*	This paper	AGD3201
C. elegans: strain AGD2281, *uthIs497[hlh-17p::hsf-1 FL::unc-54 3'UTR, myo-2p::tdTomato]*	This paper	AGD2281; in this paper *Is2(hlh-17p::hsf-1)*
C. elegans: strain AGD2290, *rmIs223[pC12C8.1::GFP; rol-6(su1006) II]*, aka AM446 backcrossed	Dillin lab and gift from Morimoto lab	AGD2290
C. elegans: strain AGD2302, *uthIs497[hlh-17p::hsf-1 FL::unc-54 3'UTR, myo-2p::tdTomato]; rmIs223[pC12C8.1::GFP; rol-6(su1006) II]*	This paper	AGD2302
C. elegans: strain AGD2293, *uthIs497[hlh-17p::hsf-1 FL::unc-54 3'UTR, myo-2p::tdTomato],dvln70[pCL25 (hsp-16.2p::GFP), pRF4(rol-6)]*	This paper	AGD2293
C. elegans: strain AGD2519, *uthEx927[fig-1p::hsf-1::unc-54 3' UTR, myo-2p::BFP]*	This paper	AGD2519
C. elegans: strain AGD2539, *uthEx927[fig-1p::hsf-1::unc-54 3' UTR, myo-2p::BFP]; dvln70[pCL25 (hsp-16.2p::GFP), pRF4(rol-6)]*	This paper	AGD2539
C. elegans: strain AGD2329,	This paper	AGD2329

uthEx904[mir-228p::hsf-1::unc-54 3' UTR, myo-2p::BFP]		
C. elegans: strain AGD2336, *uthEx904[mir-228p::hsf-1::unc-54 3' UTR, myo-2p::BFP]; dvln70[pCL25 (hsp-16.2 promoter::GFP transcriptional fusion), pRF4(rol-6)]*	This paper	AGD2336
C. elegans: strain AGD1570, *uthIs441(hlh-17p::GFP::unc-54); pRF4(rol-6)]*	Frakes et al. 2020	AGD1570
C. elegans: strain CL2166, *dvIs19[pAG15(gst-4p::GFP::NLS)] III*	CGC	CL2166
C. elegans: strain AGD2857, *uthIs497[hlh-17p::hsf-1 FL::unc-54 3'UTR, myo-2p::tdTomato]; dvIs19[pAF15(gst-4p::GFP::NLS)] III*	This paper	AGD2857
C. elegans: strain AGD 2173, backcrossed *nsIs180 (hlh-17p::recCaspase-3, unc-122p::GFP)*	Frakes et al. 2020	AGD2173
C. elegans: strain AU78, *T24B8.5p::GFP*	CGC	AU78
C. elegans: strain AGD, *uthEx861[hlh-17p::hsf-1 FL::unc-54 3'UTR, myo-2p::tdTomato]; T24B8.5p::GFP*	This paper	AGD3198
C. elegans: CZ3391 *vab-3(ju468)*	Yoshimura et al. 2008	CZ3391
C. elegans: CB648 *vab-3(e648)*	Yoshimura et al. 2008	CB648
C. elegans: LW227 *mls-2(cc615)*	Yoshimura et al. 2008	LW227
*C. elegans:*AGD2099 *vab-3(ju468); uthIs441(hlh-17p::GFP::unc-54); pRF4(rol-6)]*	This paper	AGD2099
*C. elegans:*AGD2100	This paper	AGD2100

vab-3(e648); uthIs441(hlh-17p::GFP::unc-54); pRF4(rol-6)]		
*C. elegans:*AGD2098 *mls-2(cc615); uthIs441(hlh-17p::GFP::unc-54); pRF4(rol-6)]*	This paper	AGD2098
*C. elegans:*AGD2181 *vab-3(ju468); dvln70[pCL25 (hsp-16.2p::GFP), pRF4(rol-6)]*	This paper	AGD2181
*C. elegans:*AGD3252 *vab-3(ju468); uthEx663(rab-3p::hsf-1, myo-2p::tdtomato)*	This paper	AGD3252
*C. elegans:*AGD2304 *nsIs180 (hlh-17p::recCaspase-3, unc-122p::GFP); uthIS368[rab-3p::hsf-1 FL, myo-2p::tdTomato] strain Z*	This paper	AGD2304

References

1. R. C. Taylor, A. Dillin, XBP-1 Is a Cell-Nonautonomous Regulator of Stress Resistance and Longevity. *Cell*. **153**, 1435–1447 (2013).
2. J. Labbadia, R. I. Morimoto, Repression of the Heat Shock Response Is a Programmed Event at the Onset of Reproduction. *Mol. Cell*. **59**, 639–650 (2015).
3. P. Walter, D. Ron, The unfolded protein response: From stress pathway to homeostatic regulation. *Science (80-.).* **334** (2011), pp. 1081–1086.
4. E. A. Kikis, T. Gidalevitz, R. I. Morimoto, Protein homeostasis in models of aging and age-related conformational disease. *Adv. Exp. Med. Biol.* **694**, 138–59 (2010).
5. P. M. Douglas, N. A. Baird, M. S. Simic, S. Uhlein, M. A. McCormick, S. C. Wolff, B. K. Kennedy, A. Dillin, Heterotypic Signals from Neural HSF-1 Separate Thermotolerance from Longevity. *Cell Rep.* **12**, 1196–1204 (2015).
6. C. Merkwirth, V. Jovaisaite, J. Durieux, O. Matilainen, S. D. Jordan, P. M. Quiros, K. K. Steffen, E. G. Williams, L. Mouchiroud, S. U. Tronnes, V. Murillo, S. C. Wolff, R. J. Shaw, J. Auwerx, A. Dillin, Two Conserved Histone Demethylases Regulate Mitochondrial Stress-Induced Longevity. *Cell*. **165**, 1209–1223 (2016).
7. J. Labbadia, R. I. Morimoto, The Biology of Proteostasis in Aging and Disease. *Annu. Rev. Biochem.* **84**, 435 (2015).
8. M. Daldin, V. Fodale, C. Cariulo, L. Azzollini, M. Verani, P. Martufi, M. C. Spiezia, S. M. Deguire, M. Cherubini, D. MacDonald, A. Weiss, A. Bresciani, J. P. G. Vonsattel, L. Petricca, J. L. Marsh, S. Gines, I. Santimone, M. Marano, H. A. Lashuel, F. Squitieri, A. Caricasole, Polyglutamine expansion affects huntingtin conformation in multiple Huntington's disease models. *Sci. Reports 2017 71*. **7**, 1–15 (2017).
9. Y. Hou, X. Dan, M. Babbar, Y. Wei, S. G. Hasselbalch, D. L. Croteau, V. A. Bohr, Ageing as a risk factor for neurodegenerative disease. *Nat. Rev. Neurol.* **15**, 565–581 (2019).
10. F. U. Hartl, A. Bracher, M. Hayer-Hartl, Molecular chaperones in protein folding and proteostasis. *Nat. 2011 4757356*. **475**, 324–332 (2011).
11. A. E. Frakes, A. Dillin, The UPRER: Sensor and Coordinator of Organismal Homeostasis. *Mol. Cell*. **66**, 761–771 (2017).
12. R. Higuchi-Sanabria, P. A. Frankino, J. W. Paul, S. U. Tronnes, A. Dillin, A Futile Battle? Protein Quality Control and the Stress of Aging. *Dev. Cell*. **44**, 139–163 (2018).
13. J. H. Lin, H. Li, D. Yasumura, H. R. Cohen, C. Zhang, B. Panning, K. M. Shokat, M. M. LaVail, P. Walter, IRE1 signaling affects cell fate during the unfolded protein response. *Science*. **318**, 944–949 (2007).
14. J. H. Lin, H. Li, Y. Zhang, D. Ron, P. Walter, Divergent effects of PERK and IRE1 signaling on cell viability. *PLoS One*. **4** (2009), doi:10.1371/JOURNAL.PONE.0004170.
15. E. A. Moehle, K. Shen, A. Dillin, Mitochondrial proteostasis in the context of cellular and organismal health and aging. *J. Biol. Chem.* **294**, 5396 (2019).
16. A. Vihervaara, L. Sistonen, HSF1 at a glance. *J Cell Sci*. **127**, 261–266 (2014).
17. V. Prahlad, T. Cornelius, R. I. Morimoto, Regulation of the Cellular Heat Shock Response in Caenorhabditis elegans by Thermosensory Neurons. *Science*. **320**, 811–814 (2008).
18. M. C. Tatum, F. K. Ooi, M. R. Chikka, L. Chauve, L. A. Martinez-Velazquez, H. W. M. Steinbusch, R. I. Morimoto, V. Prahlad, Neuronal serotonin release triggers the heat shock response in C. elegans in the absence of temperature increase. *Curr. Biol.* **25**, 163–174

(2015).
19. W. JG, S. E, T. JN, B. S, The structure of the nervous system of the nematode Caenorhabditis elegans. *Philos. Trans. R. Soc. Lond. B. Biol. Sci.* **314**, 1–340 (1986).
20. D. Conte, L. T. MacNei, A. J. M. Walhout, C. C. Mello, *Curr. Protoc. Mol. Biol.*, in press, doi:10.1002/0471142727.MB2603S109.
21. A. Singhvi, S. Shaham, Glia-Neuron Interactions in *Caenorhabditis elegans*. *Annu. Rev. Neurosci.* **42**, 149–168 (2019).
22. R. Bar-Ziv, A. E. Frakes, R. Higuchi-Sanabria, T. Bolas, P. A. Frankino, H. K. Gildea, M. G. Metcalf, A. Dillin, Measurements of physiological stress responses in C. elegans. *J. Vis. Exp.* **2020**, 1–21 (2020).
23. B. Estébanez, J. A. De Paz, M. J. Cuevas, J. González-Gallego, Endoplasmic Reticulum Unfolded Protein Response, Aging and Exercise: An Update. *Front. Physiol.* **9**, 1744 (2018).
24. R. Gomez-Pastor, E. T. Burchfiel, D. W. Neef, A. M. Jaeger, E. Cabiscol, S. U. McKinstry, A. Doss, A. Aballay, D. C. Lo, S. S. Akimov, C. A. Ross, C. Eroglu, D. J. Thiele, Abnormal degradation of the neuronal stress-protective transcription factor HSF1 in Huntington's disease. *Nat. Commun.* **8**, 14405 (2017).
25. E. Kim, K. Sakata, F.-F. Liao, Bidirectional interplay of HSF1 degradation and UPR activation promotes tau hyperphosphorylation. *PLOS Genet.* **13**, e1006849 (2017).
26. A. E. Frakes, M. G. Metcalf, S. U. Tronnes, R. Bar-Ziv, J. Durieux, H. K. Gildea, N. Kandahari, S. Monshietehadi, A. Dillin, Four glial cells regulate ER stress resistance and longevity via neuropeptide signaling in C. Elegans. *Science (80-.).* **367** (2020), doi:10.1126/science.aaz6896.
27. E. Sikora, A. Bielak-Zmijewska, M. Dudkowska, A. Krzystyniak, G. Mosieniak, M. Wesierska, J. Wlodarczyk, Cellular Senescence in Brain Aging. *Front. Aging Neurosci.* **13**, 71 (2021).
28. E. P. Moreno-Jiménez, J. Terreros-Roncal, M. Flor-García, A. Rábano, M. Llorens-Martín, Evidences for Adult Hippocampal Neurogenesis in Humans. *J. Neurosci.* **41**, 2541–2553 (2021).
29. A. B. Lindner, R. Madden, A. Demarez, E. J. Stewart, F. Taddei, Asymmetric segregation of protein aggregates is associated with cellular aging and rejuvenation. *Proc. Natl. Acad. Sci. U. S. A.* **105**, 3076–3081 (2008).
30. J. Durieux, S. Wolff, A. Dillin, The Cell-Non-Autonomous Nature of Electron Transport Chain-Mediated Longevity. *Cell*. **144**, 79–91 (2011).
31. R. Higuchi-Sanabria, J. W. Paul Rd, J. Durieux, C. Benitez, P. A. Frankino, S. U. Tronnes, G. Garcia, J. R. Daniele, S. Monshietehadi, A. Dillin, A. Dillin, Spatial regulation of the actin cytoskeleton by HSF-1 during aging. *Mol. Biol. Cell*. **29**, 2522–2527 (2018).
32. J. F. Morley, R. I. Morimoto, Regulation of longevity in Caenorhabditis elegans by heat shock factor and molecular chaperones. *Mol. Biol. Cell*. **15**, 657–64 (2004).
33. S. Das, F. K. Ooi, J. C. Corchado, L. C. Fuller, J. A. Weiner, V. Prahlad, Serotonin signaling by maternal neurons upon stress ensures progeny survival. *Elife*. **9** (2020), doi:10.7554/ELIFE.55246.
34. R. Higuchi-Sanabria, J. Durieux, N. Kelet, S. Homentcovschi, M. de los Rios Rogers, S. Monshietehadi, G. Garcia, S. Dallarda, J. R. Daniele, V. Ramachandran, A. Sahay, S. U. Tronnes, L. Joe, A. Dillin, Divergent Nodes of Non-autonomous UPRER Signaling through Serotonergic and Dopaminergic Neurons. *Cell Rep.* **33**, 108489 (2020).

35. K. M. Berendzen, J. Durieux, L.-W. Shao, Y. Tian, H.-E. Kim, S. Wolff, Y. Liu, A. Dillin, Neuroendocrine Coordination of Mitochondrial Stress Signaling and Proteostasis. *Cell*. **166**, 1553-1563.e10 (2016).
36. S. . Santos, M. . Saraiva, Enlarged ventricles, astrogliosis and neurodegeneration in heat shock factor 1 null mouse brain. *Neuroscience*. **126**, 657–663 (2004).
37. I. R. Brown, S. J. Rush, Cellular localization of the heat shock transcription factors HSF1 and HSF2 in the rat brain during postnatal development and following hyperthermia. *Brain Res.* **821**, 333–340 (1999).
38. R. N. Nishimura, B. E. Dwyer, K. Clegg, R. Cole, J. de Vellis, Comparison of the heat shock response in cultured cortical neurons and astrocytes. *Mol. Brain Res.* **9**, 39–45 (1991).
39. S. Mederos, C. González-Arias, G. Perea, Astrocyte–Neuron Networks: A Multilane Highway of Signaling for Homeostatic Brain Function. *Front. Synaptic Neurosci.* **10**, 45 (2018).
40. M.-È. Tremblay, B. Stevens, A. Sierra, H. Wake, A. Bessis, A. Nimmerjahn, The Role of Microglia in the Healthy Brain. *J. Neurosci.* . **31**, 16064–16069 (2011).
41. S. Mahmoud, M. Gharagozloo, C. Simard, D. Gris, Astrocytes Maintain Glutamate Homeostasis in the CNS by Controlling the Balance between Glutamate Uptake and Release. *Cells*. **8**, 184 (2019).
42. J. W. Deitmer, S. M. Theparambil, I. Ruminot, S. I. Noor, H. M. Becker, Energy Dynamics in the Brain: Contributions of Astrocytes to Metabolism and pH Homeostasis. *Front. Neurosci.* **13**, 1301 (2019).
43. S. Mason, Lactate shuttles in neuroenergetics-homeostasis, allostasis and beyond. *Front. Neurosci.* **11**, 43 (2017).
44. M. V. Sofroniew, H. V. Vinters, Astrocytes: biology and pathology. *Acta Neuropathol.* **119**, 7–35 (2010).
45. S. Kuhn, L. Gritti, D. Crooks, Y. Dombrowski, Oligodendrocytes in Development, Myelin Generation and Beyond. *Cells*. **8** (2019), doi:10.3390/CELLS8111424.
46. S. Hong, V. F. Beja-Glasser, B. M. Nfonoyim, A. Frouin, S. Li, S. Ramakrishnan, K. M. Merry, Q. Shi, A. Rosenthal, B. A. Barres, C. A. Lemere, D. J. Selkoe, B. Stevens, Complement and microglia mediate early synapse loss in Alzheimer mouse models. *Science*. **352**, 712–716 (2016).
47. D. P. Schafer, E. K. Lehrman, A. G. Kautzman, R. Koyama, A. R. Mardinly, R. Yamasaki, R. M. Ransohoff, M. E. Greenberg, B. A. Barres, B. Stevens, Microglia Sculpt Postnatal Neural Circuits in an Activity and Complement-Dependent Manner. *Neuron*. **74**, 691–705 (2012).
48. J. Rostami, S. Holmqvist, V. Lindström, J. Sigvardson, G. T. Westermark, M. Ingelsson, J. Bergström, L. Roybon, A. Erlandsson, Human Astrocytes Transfer Aggregated Alpha-Synuclein via Tunneling Nanotubes. *J. Neurosci.* **37**, 11835–11853 (2017).
49. Y. Wang, J. Cui, X. Sun, Y. Zhang, Tunneling-nanotube development in astrocytes depends on p53 activation. *Cell Death Differ. 2011 184*. **18**, 732–742 (2010).
50. I. Guzhova, K. Kislyakova, O. Moskaliova, I. Fridlanskaya, M. Tytell, M. Cheetham, B. Margulis, In vitro studies show that Hsp70 can be released by glia and that exogenous Hsp70 can enhance neuronal stress tolerance. *Brain Res.* **914**, 66–73 (2001).
51. J. A. Yin, G. Gao, X. J. Liu, Z. Q. Hao, K. Li, X. L. Kang, H. Li, Y. H. Shan, W. L. Hu, H. P. Li, S. Q. Cai, Genetic variation in glia–neuron signalling modulates ageing rate. *Nat.*

2017 5517679. **551**, 198–203 (2017).
52. S. Shaham, Glial development and function in the nervous system of Caenorhabditis elegans. *Cold Spring Harb. Perspect. Biol.* **7**, a020578 (2015).
53. Q. Zhang, X. Wu, P. Chen, L. Liu, N. Xin, Y. Tian, A. Dillin, The Mitochondrial Unfolded Protein Response Is Mediated Cell-Non-autonomously by Retromer-Dependent Wnt Signaling. *Cell*. **174**, 870-883.e17 (2018).
54. N. A. Baird, P. M. Douglas, M. S. Simic, A. R. Grant, J. J. Moresco, S. C. Wolff, J. R. Yates, G. Manning, A. Dillin, *Science (80-.).*, in press (available at http://science.sciencemag.org/content/346/6207/360.abstract).
55. K. D. Sarge, S. P. Murphy, R. I. Morimoto, Activation of heat shock gene transcription by heat shock factor 1 involves oligomerization, acquisition of DNA-binding activity, and nuclear localization and can occur in the absence of stress. *Mol. Cell. Biol.* **13**, 1392–1407 (1993).
56. I. Mori, Y. Ohshima, Neural regulation of thermotaxis in Caenorhabditis elegans. *Nat. 1995 3766538*. **376**, 344–348 (1995).
57. F. K. Ooi, V. Prahlad, Olfactory learning primes the heat shock transcription factor HSF-1 to enhance the expression of molecular chaperone genes in C. elegans. *bioRxiv*, 1–18 (2017).
58. Y. C. Chen, H. J. Chen, W. C. Tseng, J. M. Hsu, T. T. Huang, C. H. Chen, C. L. Pan, A C. elegans Thermosensory Circuit Regulates Longevity through crh-1/CREB-Dependent flp-6 Neuropeptide Signaling. *Dev. Cell*. **39**, 209–223 (2016).
59. S. Speese, M. Petrie, K. Schuske, M. Ailion, K. Ann, K. Iwasaki, E. M. Jorgensen, T. F. J. Martin, UNC-31 (CAPS) Is Required for Dense-Core Vesicle But Not Synaptic Vesicle Exocytosis in Caenorhabditis elegans (2007), doi:10.1523/JNEUROSCI.1466-07.2007.
60. J. E. Richmond, W. S. Davis, E. M. Jorgensen, UNC-13 is required for synaptic vesicle fusion in C. elegans. *Nat. Neurosci. 1999 211*. **2**, 959–964 (1999).
61. S. Asikainen, S. Vartiainen, M. Lakso, R. Nass, G. Wong, Selective sensitivity of Caenorhabditis elegans neurons to RNA interference. *Neuroreport*. **16**, 1995–1999 (2005).
62. D. Kovács, T. Sigmond, B. Hotzi, B. Bohár, D. Fazekas, V. Deák, T. Vellai, J. Barna, HSF1Base: A Comprehensive Database of HSF1 (Heat Shock Factor 1) Target Genes. *Int. J. Mol. Sci.* **20** (2019), doi:10.3390/IJMS20225815.
63. J. Li, L. Chauve, G. Phelps, R. M. Brielmann, R. I. Morimoto, E2F coregulates an essential HSF developmental program that is distinct from the heat-shock response. *Genes Dev.* **30**, 2062–2075 (2016).
64. I. S. Singh, J. R. He, S. Calderwood, J. D. Hasday, A high affinity HSF-1 binding site in the 5'-untranslated region of the murine tumor necrosis factor-alpha gene is a transcriptional repressor. *J. Biol. Chem.* **277**, 4981–4988 (2002).
65. E. Eden, R. Navon, I. Steinfeld, D. Lipson, Z. Yakhini, GOrilla: a tool for discovery and visualization of enriched GO terms in ranked gene lists. *BMC Bioinformatics*. **10**, 48 (2009).
66. E. Eden, D. Lipson, S. Yogev, Z. Yakhini, Discovering Motifs in Ranked Lists of DNA Sequences. *PLOS Comput. Biol.* **3**, e39 (2007).
67. Y. Zhao, A. F. Gilliat, M. Ziehm, M. Turmaine, H. Wang, M. Ezcurra, C. Yang, G. Phillips, D. McBay, W. B. Zhang, L. Partridge, Z. Pincus, D. Gems, Two forms of death in ageing Caenorhabditis elegans. *Nat. Commun. 2017 81*. **8**, 1–8 (2017).
68. V. Singh, A. Aballay, Heat-shock transcription factor (HSF)-1 pathway required for

Caenorhabditis elegans immunity. *Proc. Natl. Acad. Sci.* **103**, 13092–13097 (2006).
69. K. A. Guttenplan, M. K. Weigel, P. Prakash, P. R. Wijewardhane, P. Hasel, U. Rufen-Blanchette, A. E. Münch, J. A. Blum, J. Fine, M. C. Neal, K. D. Bruce, A. D. Gitler, G. Chopra, S. A. Liddelow, B. A. Barres, Neurotoxic reactive astrocytes induce cell death via saturated lipids. *Nat. 2021 5997883*. **599**, 102–107 (2021).
70. F. Wang, H. B. Bradshaw, S. Pena, B. Jablonska, J. Xavier, S. Gong, B. Li, D. Chandler-Militello, L. K. Bekar, N. A. Smith, *bioRxiv*, in press, doi:10.1101/2020.01.12.903393.
71. M. S. Ioannou, J. Jackson, S. H. Sheu, C. L. Chang, A. V. Weigel, H. Liu, H. A. Pasolli, C. S. Xu, S. Pang, D. Matthies, H. F. Hess, J. Lippincott-Schwartz, Z. Liu, Neuron-Astrocyte Metabolic Coupling Protects against Activity-Induced Fatty Acid Toxicity. *Cell*. **177**, 1522-1535.e14 (2019).
72. M. Katz, F. Corson, W. Keil, A. Singhal, A. Bae, Y. Lu, Y. Liang, S. Shaham, Glutamate spillover in C. elegans triggers repetitive behavior through presynaptic activation of MGL-2/mGluR5. *Nat. Commun. 2019 101*. **10**, 1–13 (2019).
73. A. Brunet, A. Bonni, M. J. Zigmond, M. Z. Lin, P. Juo, L. S. Hu, M. J. Anderson, K. C. Arden, J. Blenis, M. E. Greenberg, Akt Promotes Cell Survival by Phosphorylating and Inhibiting a Forkhead Transcription Factor. *Cell*. **96**, 857–868 (1999).
74. X. Sun, W. D. Chen, Y. D. Wang, DAF-16/FOXO transcription factor in aging and longevity. *Front. Pharmacol.* **8**, 548 (2017).
75. K. Lin, H. Hsin, N. Libina, C. Kenyon, Regulation of the Caenorhabditis elegans longevity protein DAF-16 by insulin/IGF-1 and germline signaling. *Nat. Genet. 2001 282*. **28**, 139–145 (2001).
76. V. Singh, A. Aballay, Heat Shock and Genetic Activation of HSF-1 Enhance Immunity to Bacteria. *http://dx.doi.org/10.4161/cc.5.21.3434*. **5**, 2443–2446 (2006).
77. D. Garigan, A. L. Hsu, A. G. Fraser, R. S. Kamath, J. Abringet, C. Kenyon, Genetic Analysis of Tissue Aging in Caenorhabditis elegans: A Role for Heat-Shock Factor and Bacterial Proliferation. *Genetics*. **161**, 1101–1112 (2002).
78. A. E. Frakes, M. G. Metcalf, S. U. Tronnes, R. Bar-Ziv, J. Durieux, H. K. Gildea, N. Kandahari, S. Monshietehadi, A. Dillin, Four glial cells regulate ER stress resistance and longevity via neuropeptide signaling in C. Elegans. *Science (80-.).* **367**, 436–440 (2020).
79. E. Afgan, D. Baker, M. van den Beek, D. Blankenberg, D. Bouvier, M. Čech, J. Chilton, D. Clements, N. Coraor, C. Eberhard, B. Grüning, A. Guerler, J. Hillman-Jackson, G. Von Kuster, E. Rasche, N. Soranzo, N. Turaga, J. Taylor, A. Nekrutenko, J. Goecks, The Galaxy platform for accessible, reproducible and collaborative biomedical analyses: 2016 update. *Nucleic Acids Res.* **44**, W3–W10 (2016).
80. E. Eden, R. Navon, I. Steinfeld, D. Lipson, Z. Yakhini, GOrilla: A tool for discovery and visualization of enriched GO terms in ranked gene lists. *BMC Bioinformatics*. **10**, 1–7 (2009).
81. C. E. Grant, T. L. Bailey, W. S. Noble, FIMO: scanning for occurrences of a given motif. *Bioinformatics*. **27**, 1017 (2011).
82. T. L. Bailey, J. Johnson, C. E. Grant, W. S. Noble, The MEME Suite. *Nucleic Acids Res.* **43**, W39–W49 (2015).
83. K. L. Howe, B. J. Bolt, M. Shafie, P. Kersey, M. Berriman, WormBase ParaSite − a comprehensive resource for helminth genomics. *Mol. Biochem. Parasitol.* **215**, 2–10 (2017).
84. A. Sandelin, W. Alkema, P. Engström, W. W. Wasserman, B. Lenhard, JASPAR: an

open-access database for eukaryotic transcription factor binding profiles. *Nucleic Acids Res.* **32**, D91–D94 (2004).

85. M. Wang, Y. He, T. J. Sejnowski, X. Yu, Brain-state dependent astrocytic Ca2+ signals are coupled to both positive and negative BOLD-fMRI signals. *Proc. Natl. Acad. Sci. U. S. A.* **115**, E1647–E1656 (2018).
86. S. Shaham, Glia–neuron interactions in the nervous system of Caenorhabditis elegans. *Curr. Opin. Neurobiol.* **16**, 522–528 (2006).
87. D. A. Colón-Ramos, M. A. Margeta, K. Shen, Glia Promote Local Synaptogenesis Through UNC-6 (Netrin) Signaling in C. elegans. *Science*. **318**, 103 (2007).
88. W. Fung, L. Wexler, M. G. Heiman, Cell-type-specific promoters for C. elegans glia. *J. Neurogenet.* (2020), doi:10.1080/01677063.2020.1781851/SUPPL_FILE/INEG_A_1781851_SM0486.PDF.
89. S. Yoshimura, J. I. Murray, Y. Lu, R. H. Waterston, S. Shaham, mls-2 and vab-3 control glia development, hlh-17/Olig expression and glia-dependent neurite extension in C. elegans. *Development*. **113**, 755–765 (2008).
90. M. Katz, F. Corson, S. Iwanir, D. Biron, S. Shaham, Glia Modulate a Neuronal Circuit for Locomotion Suppression during Sleep in C. elegans. *Cell Rep.* **22**, 2575–2583 (2018).
91. C. M. Felton, C. M. Johnson, Modulation of dopamine-dependent behaviors by the Caenorhabditis elegans Olig homolog HLH-17. *J. Neurosci. Res.* **89**, 1627–1636 (2011).